Case Report

Unprecedented Persistence of Vaccine mRNA, Plasmid DNA, Spike Protein, and Genomic Dysregulation Over 3.5 Years Post-COVID-19 mRNA Vaccination

Nicolas Hulscher, MPH [1]*, Vanessa Schmidt, PhD [2], Michael Mörz, MD[3], Claire Rogers, PA-C [1], Natalia von Ranke, PhD [4], Wei Zhang, PhD [4], John A. Catanzaro ND, PhD [4], Peter A. McCullough MD, MPH [1]

[1]McCullough Foundation, Dallas, TX

[2]Inmodia GmbH, Institute for Molecular Diagnostics, Wittgasse 9, 94032 Passau, Germany

[3]Institute of Pathology 'Georg Schmorl', The Municipal Hospital Dresden-Friedrichstadt, Friedrichstrasse 41, 01067 Dresden, Germany.

[4]Neo7Bioscience, Inc, Dallas, TX

*Correspondence: nichulscher@gmail.com (Nicolas Hulscher)

Funding Statement: No funding was received for conducting this case study.

Informed Consent Statement: Written informed consent was obtained from the patient for publication of this case report and accompanying images.

Conflicts of Interest Statement: The authors declare no conflict of interest.

Acknowledgements: None.

Word Count: 10814

Abstract

Background: The long-term bio-distribution and persistence of components from COVID-19 RNA vaccines remain insufficiently characterized. Emerging evidence suggests that prolonged spike protein expression, residual RNA, and plasmid DNA fragments may contribute to multi-system post-vaccination syndromes.

Case Presentation: We report a 55-year-old male who received three doses of the Pfizer–BioNTech COVID-19 mRNA vaccine and subsequently developed progressive multi-organ dysfunction consistent with post-COVID-19 vaccine syndrome (PCVS), involving cardiopulmonary, neurologic, musculoskeletal, gastrointestinal, autonomic, otolaryngologic, audiovestibular, immune, ophthalmic, dermatologic, and psychiatric domains. Clinical manifestations included: pulmonary emboli; delayed MRI-confirmed myocarditis; neurocognitive impairment; small fiber neuropathy; autonomic dysfunction; myalgia; chronic pancreatic and gastrointestinal involvement; worsened tinnitus with sensorineural hearing loss; voice dysphagia and dysphonia; ophthalmic disturbances; chronic dermatologic inflammation; and anxiety/depression. The case was evaluated through a uniquely extensive longitudinal, multi-domain clinical investigation spanning molecular, immunologic, genetic, proteomic, transcriptomic, and tissue-based analyses, undertaken to characterize disease mechanisms and exclude alternative etiologies.

Diagnostic Evaluation: After >40 emergency department visits and >200 outpatient specialty encounters, the patient underwent >100 non-routine laboratory investigations and >100 imaging/functional studies. This evaluation systematically excluded underlying etiologic mechanisms across infectious, autoimmune, rheumatologic, endocrine, genetic, hematologic, malignant, toxic/medication-related, cardiovascular/vascular, metabolic, and primary neurologic domains. Testing remained largely nondiagnostic. A possible undocumented/undiagnosed asymptomatic infection manifesting as Long COVID was suspected after myocarditis diagnosis, and serology was pursued; unexpected results prompted expanded immune and tissue-based testing for spike- and vaccine-derived components. SARS-CoV-2 nucleocapsid antibodies were negative across five separate time points spanning 809–1,433 days post-vaccination, confirmed by three independent laboratories. The patient remains nucleocapsid negative with persistently elevated spike antibody levels (4,553 U/mL) 1,433 days after the final vaccination.

Specimen Collection and Analytical Methods: Blood and skin tissue specimens were obtained at multiple time points between 852–1,364 days after the final Pfizer–BioNTech COVID-19 mRNA vaccination. Biological compartments analyzed included plasma, circulating exosomes, peripheral blood mononuclear cells (PBMCs), and skin tissue. Specimens were evaluated across multiple independent laboratories using diverse analytical methodologies, including ELISA, automated immunohistochemistry, RT-PCR, standard PCR with Sanger sequencing confirmation, whole-genome sequencing, transcriptomic profiling, and quantitative mass spectrometry.

Circulating Molecular Findings: At 852 days post-vaccination, blood-based immune testing identified detectable SARS-CoV-2 S1 protein within classical and non-classical monocyte subsets with associated cytokine and immune marker abnormalities. At 1,173 days post-vaccination, high-sensitivity ELISA detected free Wuhan spike protein in plasma (129.0 ± 4.1 fg/mL) and in circulating exosomes (11.6 ± 0.1 fg/mL). At 1,284 days, RT-PCR identified vaccine-derived spike mRNA within circulating exosomes, whereas PBMC RNA remained negative following DNase-treated extraction and amplicon-specific PCR targeting three spike ORF regions (S1–S3). Serologic profiling at 1,173 and 1,284 days post-vaccination demonstrated persistently elevated spike-specific IgG4 concentrations (354.4 ± 22.4 ng/mL and 320.2 ± 4.4 ng/mL, respectively), consistent with ongoing antigenic stimulation and an immune-tolerance–skewed response.

Tissue-Level Molecular and Histopathologic Findings: Serial skin biopsies at 1,160, 1,249, and 1,364 days post-vaccination, all from truncal skin within areas of clinically active Grover's disease, were nucleocapsid negative and demonstrated persistent spike protein deposition in endothelial cells and macrophages by automated immunohistochemistry with histopathologic correlation. Spike protein was also found in nerve fibers at 1,364 days. The 1,364-day skin biopsy contained multiple plasmid DNA elements, including spike gene sequences (S1–S3), ori1/ori2, and the SV40 enhancer, confirming durable retention of vaccine-derived DNA in somatic tissue by PCR amplification with agarose gel electrophoresis and Sanger sequencing.

Multi-Omic Analysis: Whole-genome sequencing structural variant analysis at 1,277 days post-vaccination revealed widespread genomic instability, with large duplications and deletions affecting EGFR, MYC, ERBB2, and ETV6/RUNX1, while RNA–DNA comparison showed RNA-only variants in ribosomal, NMD, small-RNA, epigenetic, and TP53 pathways. Transcriptomic profiling of whole blood highlighted oxidative stress, vascular activation, and nuclear fragility. Urine proteomics using quantitative mass spectrometry confirmed systemic inflammation with complement overactivation (CFH), redox imbalance (PRDX1), and sustained antibody responses, supported by risk alleles HLA-B07:02 and DRB1*11:04.

Conclusion: This case documents the longest reported in vivo persistence of vaccine-derived mRNA, plasmid DNA fragments, and spike protein following mRNA vaccination, with reproducible detection across multiple independent laboratories, distinct biological compartments, and complementary molecular detection systems extending beyond 3.5 years after the final dose. Spike protein, spike mRNA sequences, and plasmid backbone elements were identified in both immune cells and somatic tissue, with continued absence of SARS-CoV-2 nucleocapsid protein or antibodies, effectively excluding prior infection as the source. The convergence of these observations across longitudinal blood and tissue sampling provides direct evidence that mRNA vaccine-derived genetic material and its translated protein products can persist in vivo for years following administration. In parallel, multi-omic analyses revealed sustained genomic instability and transcriptomic dysregulation more than 3.5 years post-vaccination, suggesting that persistent vaccine-derived material may be associated with long-term alterations in host genomic and molecular pathways. These data challenge prevailing assumptions regarding rapid degradation and short-lived biological activity of mRNA vaccine components and underscore the need for controlled longitudinal studies to determine prevalence, mechanisms, and clinical consequences of persistent vaccine-derived material.

Introduction

COVID-19 mRNA vaccines were rapidly distributed by the United States government under Emergency Use Authorization in late 2020 due to the global spread of SARS-CoV-2 [1]. Because clinical trials had not been completed at the time of distribution, the potential adverse effects were unknown. Of particular importance were the unknown implications for the encoding of the highly inflammatory spike protein, one of the most toxic components of the COVID-19 virus[2,3]. Lipid nanoparticle (LNP) encapsulated vaccine mRNA has been found to penetrate the human brain [4] and heart [5]. After the LNP deposits in various organs throughout the body [6], the spike protein is then expressed within those cells for an unknown duration resulting in an inflammatory response in that organ system [2]. As a result, patients experiencing post-COVID-19 vaccine syndrome (PCVS) present with a myriad of symptoms involving multiple organ systems [7]. Myocarditis is now recognized as a serious adverse reaction to the COVID-19 vaccine, most frequently in young adult males, but not limited to this group [8]. The mechanism is thought to be due to spike protein accumulation in cardiomyocytes leading to inflammation, the potential for subsequent scarring, and, ultimately, damage to the heart muscle [8]. Here, we report a case of multi-system post–COVID-19 vaccination syndrome supported by a uniquely extensive longitudinal molecular, immunologic, genetic, proteomic, transcriptomic, and tissue-level assessment.

Case Presentation

Patient is a 55-year-old male with a history of postoperative venous thromboembolism, complicated by deep venous thrombosis and pulmonary embolism at age 46 following lumbar spine surgery. He completed three months of anticoagulation, with follow-up imaging demonstrating resolution; thrombophilia evaluation was unremarkable. Past medical history included mild hearing loss with tinnitus, intermittently elevated blood pressure treated at times with low-dose losartan, and occasional anxiety. Prior routine physical examinations, coronary calcium scoring, and a baseline cardiac stress test were reported as normal.

Vaccination and Early Systemic Symptoms

The patient received a two-dose Pfizer–BioNTech COVID-19 mRNA vaccination series in March 2021. Beginning in May 2021, he developed episodic systemic symptoms including body aches, headaches, fatigue, and bloating, followed by intermittent ENT complaints (sore throat, poor sleep, and a sensation of ear fluid). During fall 2021, he developed persistent low-grade chest pain (typically ~2/10), fatigue/malaise, and shortness of breath, prompting outpatient evaluation prior to his first emergency department visit. On October 28, 2021, he presented to the emergency department with abrupt, self-resolving tachycardia (heart rate ~208 bpm) accompanied by dizziness, disorientation, shortness of breath, difficulty focusing, and diplopia. Testing was limited, and symptoms were attributed to anxiety.

Pulmonary Embolism and Follow-Up

He re-presented to the emergency department on November 8, 2021, with tachycardia and shortness of breath; laboratory testing demonstrated an elevated D-dimer of 1.71 µg/mL FEU (reference range <0.22 µg/mL FEU). Chest CT on November 9, 2021 demonstrated multiple small bilateral pulmonary emboli, prompting hospitalization, specialty referral, and initiation of anticoagulation (**Figure 1**).

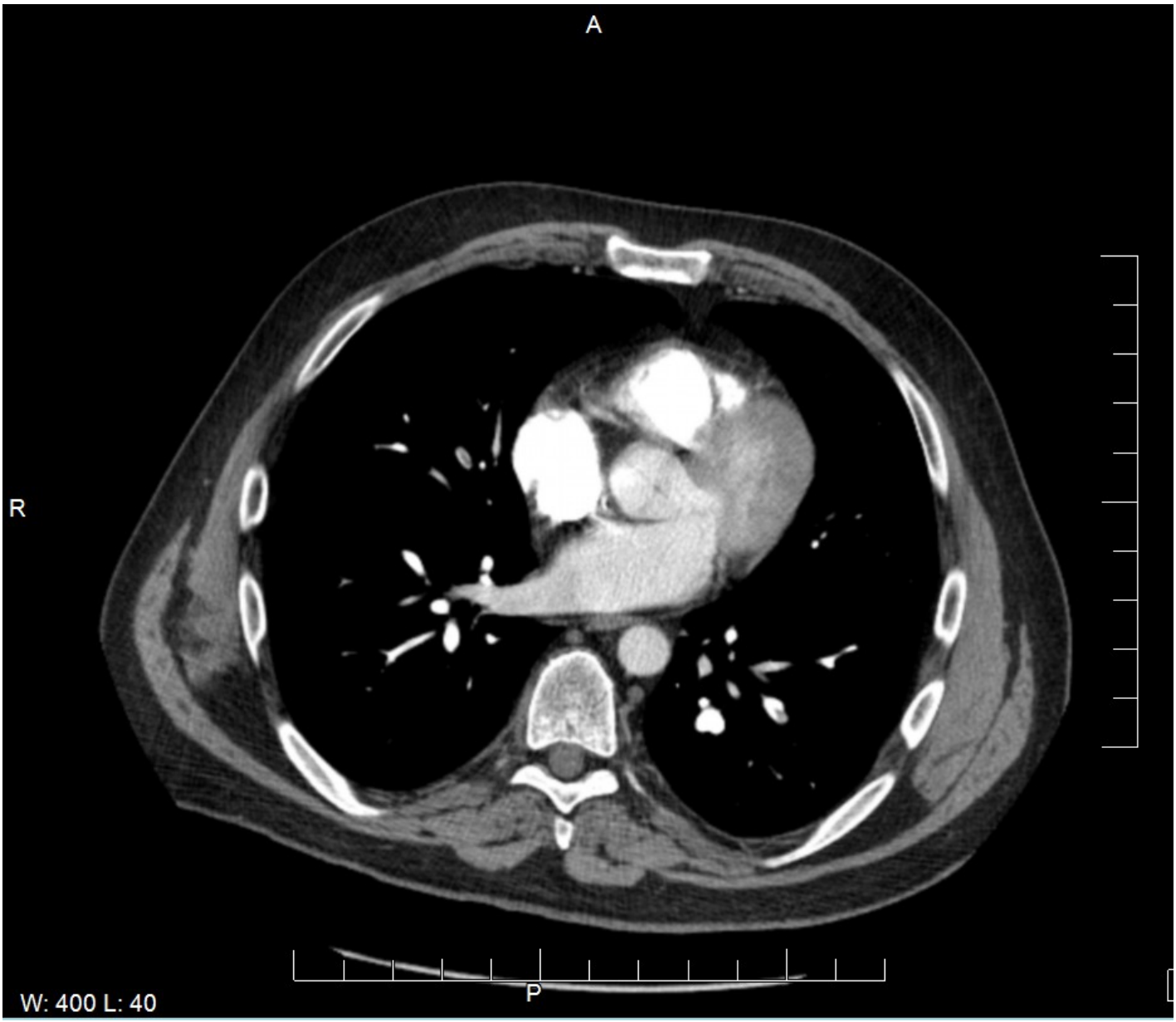

Figure 1. Computed Tomography (CT) Pulmonary Angiogram Demonstrating Pulmonary Embolism. Axial CT pulmonary angiogram image dated November 9, 2021, showing multiple small pulmonary emboli in the segmental and subsegmental branches of the left pulmonary artery. The emboli appear as intraluminal filling defects within contrast-opacified pulmonary arteries, consistent with acute pulmonary embolism. This diagnosis occurred approximately eight months following the patient's second dose of the Pfizer-BioNTech COVID- 19 mRNA vaccine.

Two thrombophilia evaluations (January 2022 and December 2022) were unremarkable. The patient received a Pfizer-BioNTech mRNA booster on February 20, 2022; chest CT on February 22, 2022 demonstrated resolution of the pulmonary emboli and described clear lungs without inflammatory findings. Symptoms persisted and broadened across multiple systems.

Post-booster multi-system escalation

After the February 20, 2022 Pfizer-BioNTech mRNA booster, the patient reported multisystem symptom escalation, with onset in March–April 2022 and more pronounced tachycardic, gastrointestinal, autonomic, and neuropsychiatric episodes by May 2022. Symptoms included headaches with dizziness and intermittent diplopia/visual disturbance; worsening tinnitus with bilateral sensorineural hearing loss; bloating and abdominal pain; worsening chest pain with exertional intolerance; tachycardia with hypotension and near-syncope; musculoskeletal pain disproportionate to exertion; and new severe anxiety. Hematospermia with

prostatitis was diagnosed in March 2022. During this period, symptoms were frequently attributed to anxiety in the post–pulmonary embolism setting.

In July 2022, chest CT showed no recurrent pulmonary emboli but demonstrated new scattered semi-solid ground-glass opacities described as suggestive of infection or inflammation; the patient denied infectious symptoms at that time. This contrasted with a clear chest CT in February 2022.

Cardiology

Between 2022 and 2024, the patient underwent extensive cardiac evaluation, including multiple transthoracic echocardiograms demonstrating normal cardiac chamber size and preserved systolic function; multiple exercise stress tests and stress echocardiograms that were electrocardiographically and echocardiographically normal but clinically symptomatic (chest pain, dyspnea, dizziness, and prolonged heart rate recovery); and serial ambulatory rhythm monitoring demonstrating occasional premature atrial contractions (PACs), occasional premature ventricular contractions (PVCs), and brief self-terminating supraventricular tachycardia (SVT).

On May 28, 2023, the patient captured self-terminating runs of idioventricular rhythm (**Figure 2**) on a home monitoring device during an episode of severe chest pain; the rhythm strip was verified by a medical provider. This finding did not prompt escalation to advanced cardiac imaging. During this period, myocarditis and pericarditis were mentioned in emergency department differentials; however, the patient was reassured that these diagnoses were unlikely, despite no cardiac MRI being performed.

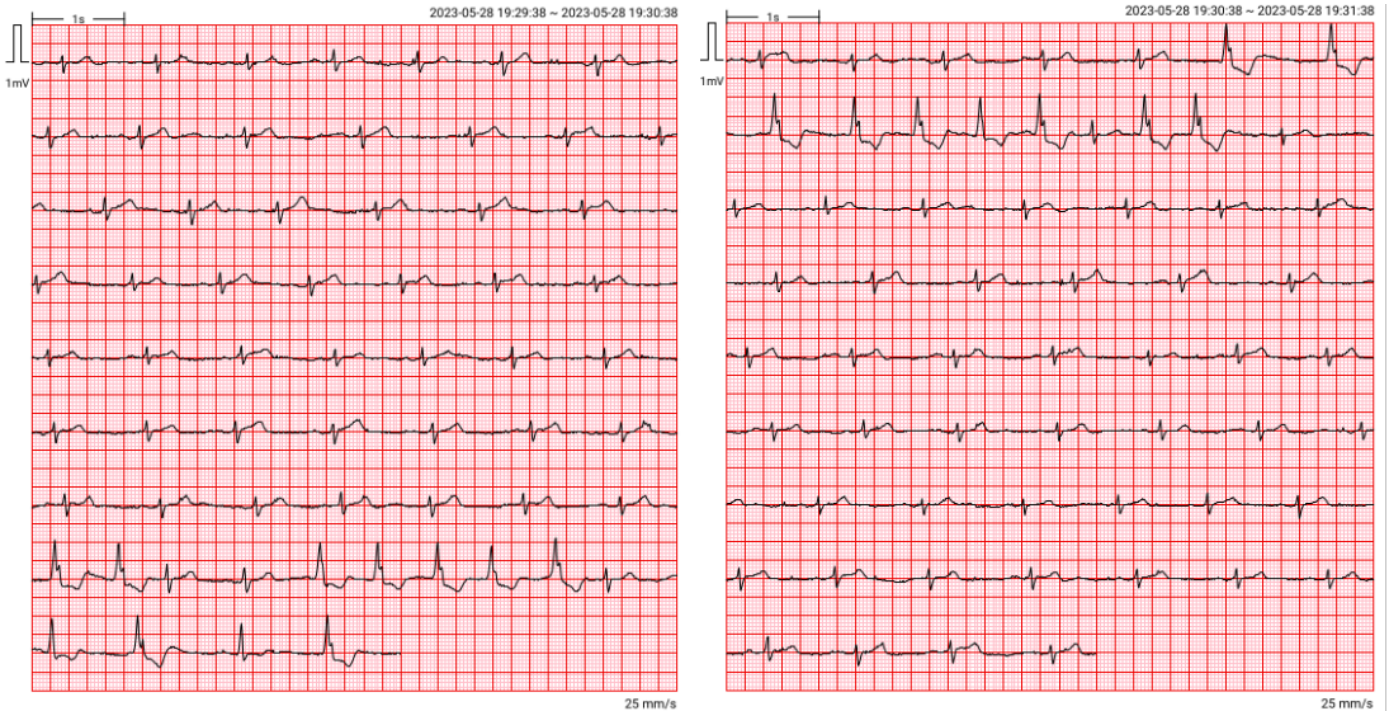

Figure 2. Intermittent Idioventricular Rhythm Captured on Ambulatory ECG Monitoring (May 28, 2023)

From 2021–2024, he had >35 emergency department visits and ~30 cardiology visits (conservative counts), predominantly for chest pain, shortness of breath, dizziness, or palpitations. During this interval, he underwent >40 complete blood counts (CBCs), >40 comprehensive metabolic panels (CMPs), >40 troponin measurements, and 13 B-type natriuretic peptide (BNP) measurements, which were documented as consistently within reference range, with the exception of low anion gap. The most frequent emergency department discharge diagnoses during this period were atypical chest pain and anxiety.

On April 9, 2024 (approximately two and a half years after symptom onset), a cardiac MRI was ordered by cardiology, which found the presence of inflammation and mild scarring consistent with COVID-19 vaccine-induced myocarditis (**Figure 3**). This diagnosis was then confirmed by a cardiac specialist. A comprehensive genetic profile for arrhythmias and cardiomyopathies was negative. After the myocarditis diagnosis, the evaluation shifted toward identifying a unifying etiology.

Figure 3. Cardiac MRI Demonstrating Myocardial Inflammation Consistent with Vaccine- Induced Myocarditis. Axial T1-weighted cardiac magnetic resonance image (MRI) with late gadolinium enhancement (LGE), dated April 9, 2024, demonstrating subepicardial and mid-myocardial signal hyperintensity in the lateral wall of the left ventricle—findings consistent with myocarditis. This radiologic pattern is characteristic of non-ischemic myocardial inflammation.

Over the same period, symptoms extended beyond cardiopulmonary complaints and were evaluated across multiple organ systems; in several domains, symptoms preceded formal diagnoses and were assessed repeatedly over time. Key findings are summarized below by organ system.

Gastroenterology

Symptoms and Initial GI Evaluation

Gastroenterology evaluation on August 1, 2022 documented hoarseness/dry throat, abdominal pain, chest pain, bloating, belching, gas, and change in bowel habits.

Upper GI and Esophageal Motility

Upper endoscopy on October 17, 2022 demonstrated an irregular Z-line at 40 cm from the incisors, diffuse mild gastric erythema, and a 2 cm sliding hiatal hernia. On May 17, 2023, repeat upper endoscopy demonstrated no hiatal hernia, an irregular Z-line, Hill grade II valve, no esophagitis, and gastritis, with normal duodenum and jejunum. Esophagram demonstrated contrast stasis (no solid-phase study performed). High-resolution manometry demonstrated 100% ineffective esophageal motility (60% failed swallows, 40% weak

swallows). BRAVO pH monitoring was incomplete due to probe detachment on day 2. Esophageal and duodenal biopsies were negative during these evaluations. Reported symptoms were noted to worsen with eating and exercise, with primary symptoms including chest discomfort/chest pain, difficulty taking deep breaths, and left subcostal pain.

Dysbiosis and Microbiome

The patient reported bloating, constipation, belching, and abdominal pain. Initial breath testing for small intestinal bacterial overgrowth (SIBO) in July 2023 using a lactulose-based TrioSmart protocol demonstrated a hydrogen rise ≥20 ppm within 100 minutes, consistent with SIBO. Multiple repeat TrioSmart tests through 2024 following attempted therapies demonstrated persistent elevation (non-response). IBS-Smart testing on October 9, 2023 demonstrated anti-CdtB and anti-vinculin antibodies not elevated. The patient reported lack of response to rifaximin and elemental diet and discontinued rifaximin/neomycin due to worsening tinnitus and sensorineural hearing loss; motegrity was used to support motility. Notably, hydrogen-predominant breath test patterns are more commonly associated with diarrhea-predominant presentations, whereas this patient's predominant bowel pattern was constipation. Concurrent esophageal dysmotility was documented during this period in the setting of ongoing gastrointestinal symptoms.

Two stool analyses were performed in 2024. One reported loss of normal enteric flora. In February 2024, a comprehensive stool analysis demonstrated increased Bacteroides family with decreased Bifidobacterium, elevated secretory IgA (326 mg/dL; reference range 30–275), and short-chain fatty acid abnormalities (decreased acetate %, increased butyrate %, and increased valerate %). The Bacteroides increase with Bifidobacterium reduction has been described by Hazan et al. following mRNA COVID-19 vaccination [9].

Lower GI and Colonoscopy Surveillance

The patient's initial colonoscopy on October 17, 2022 demonstrated diverticulosis and multiple colon polyps (one 15 mm cecal polyp and nine 4–8 mm polyps in the transverse/ascending colon). Notably, a 6-month surveillance colonoscopy on April 12, 2023, demonstrated diverticulosis (sigmoid and descending colon) and polyps (one 6 mm sessile polyp in the ascending colon and eight diminutive sessile polyps across the sigmoid, descending, transverse colon, and cecum). Surveillance intervals were subsequently adjusted to 1 year after the April 2023 colonoscopy; a 2024 colonoscopy was negative, after which follow-up was extended to 1.5 years. Across these evaluations, all polyps were resected and biopsies were negative. Genetic testing was performed (Invitae Adenomatous Polyposis Panel and Invitae Multi-Cancer testing with RNA analysis), and no pathogenic variants were identified.

Pancreatic Enzymes and Capsule Endoscopy

Capsule endoscopy on February 28, 2024 demonstrated small scattered non-bleeding angioectasia without active bleeding. Recurrent pancreatic enzyme abnormalities were documented from October 2023 through October 2025 (serial amylase/lipase elevations, including isoenzyme testing on September 25, 2025); isoenzyme testing supported a pancreatic source. Chronic pancreatitis was listed as a working diagnosis and an endoscopic ultrasound was scheduled.

Of note, the patient lost ~50 lbs from 04/2022 to 04/2024 (~21% of body weight) and was not on a weight-loss medication.

Otolaryngology / Laryngology

Otolaryngology evaluation on 03/22/2022 documented worsening tinnitus and audiologic testing showing high-frequency hearing loss, with bilateral sensorineural hearing loss that was asymmetric and worse in the right ear (right moderate to severe; left mild to moderate). Between Spring 2022 and Fall 2025, the record documents at least six audiologic hearing tests (conservative count), with earlier interval worsening followed by subsequent stability, and the most recent test in Fall 2025.

Multiple evaluations beginning August 2022 documented laryngospasm, reflux without esophagitis, and oropharyngeal dysphagia, with additional documentation of vocal fold inflammation and voice dysphonia. A laryngology evaluation on 02/06/2024 (videostroboscopy) documented mild to moderate vocal fold atrophy.

Intermittent dizziness was documented as part of the otolaryngology-related symptom history. Benign paroxysmal positional vertigo (BPPV) was documented in neurology records (2022–2024).

Neurology and structural imaging

A neurology visit on 04/18/2022 documented headaches, tinnitus/hearing issues, dizziness, confusion, paresthesias, weakness, and sleep disturbance. Symptoms were subsequently described as progressive, without a clear etiology.

A referral to academic neurology was documented in 06/2023 for multiple neurologic symptoms of unclear etiology; EMG/NCS with repetitive nerve stimulation (06/29/2023) was normal. Between 2022–2024, neurology documentation included three episodes of BPPV.

In February 2025, documentation described an episode of painless right foot drop (Emergency Department impression: peroneal nerve injury vs L5 radiculopathy) and later right elbow numbness; the workup was described as unrevealing, and additional screening was

noted as negative for myasthenia gravis and giant cell arteritis. At follow-up, interval history documented persistent dizziness/disequilibrium, tinnitus, autonomic symptoms, diplopia/visual complaints, dysphagia, cognitive fog, fatigue, hypotension, temperature intolerance, exercise intolerance, and progressive left-sided tightness/pain; the neurologic examination was nonfocal. On 04/24/2025, a nerve punch biopsy supported a clinical assessment of small fiber neuropathy and myalgia.

Structural imaging (10/2023–02/2025): MRI studies reported multilevel degenerative disc disease (cervical/thoracic/lumbar) with moderate–severe canal narrowing at C5–C6, osseous vertebral hemangiomas (T1/T3 ± T4), bilateral hip cartilage loss, and mild left hamstring tendinosis; shoulder MRI reported rotator cuff tendinopathy with near–full thickness supraspinatus tear.

Across evaluations by orthopedics, neurology, neuromuscular medicine, and neurosurgery examinations were documented as nonfocal, and EMG/NCS was documented as normal.

Dermatology

Dermatology documentation described orange-yellow facial papules with telangiectasia on 08/30/2021, which resolved over Fall 2021. A trunk rash was documented on 11/08/2022. Between 2022–2025, the record documents multiple visits for rash in which the condition was not definitively diagnosed, and topical therapies were attempted. A punch skin biopsy on 04/14/2025 (left lateral abdomen) reported pathology consistent with transient acantholytic dermatosis (Grover's disease) (**Figure 4**).

Figure 4. Grover's Disease (Transient Acantholytic Dermatosis) Following COVID-19 mRNA Vaccination. Clinical photograph taken in March 2022 depicting scattered erythematous papules and crusted lesions on the upper torso, consistent with Grover's disease

(transient acantholytic dermatosis). Diagnosis was confirmed by dermatopathology. Symptoms emerged within weeks of the patient's third Pfizer-BioNTech COVID-19 mRNA vaccine dose and were accompanied by systemic inflammatory signs, including myocarditis and gastrointestinal dysfunction. Serial skin biopsies from clinically affected trunk skin (all obtained from areas demonstrating active Grover's disease lesions) more than three years post-vaccination demonstrated persistent detection of spike protein by immunohistochemistry, with absence of SARS-CoV-2 nucleocapsid protein in all specimens. The 1,364-day biopsy additionally demonstrated PCR-detectable spike gene fragments (S1–S3), origin-of-replication sequences (ori1/ori2), and SV40 enhancer sequences in extracted tissue DNA, with Sanger sequencing confirmation of replication-origin fragments.

Urology

On 03/22/2022, prostatitis with hematospermia was diagnosed. Between 2022–2025, multiple PSA tests and multiple urine tests reported as negative.

Ophthalmology

Visual symptoms were evaluated beginning 04/05/2022, with documentation of vision fluctuation and headaches (symptoms reported as beginning ~2 months prior), along with dryness and decreased vision. Impressions included bilateral dry eye, macular scars (OS; post-inflammatory/traumatic), RPE hypopigmentation, and benign choroidal neoplasm (OD). On 06/07/2022, follow-up documentation included worsening vision fluctuations (L>R) with intermittent horizontal diplopia, dizziness, and photophobia, with assessment documenting suspected decompensated phoria and worsened dry eye. Night vision issues were reported.

An ophthalmology visit in May 2024 included left eye pain and vision described as "off," with exam findings documenting bilateral retinal hemorrhages (superior; resolving), dry eye, and blepharitis. Esotropia with divergence insufficiency was diagnosed in April 2025.

Psychiatry / Mental Health

Psychiatric care began on 02/09/2022 for anxiety symptoms described as atypical in character and intensity. A trial of escitalopram (mid-05/2022) was associated with tachycardia and uncontrolled shaking and was assessed during an emergency visit as possible serotonin syndrome. Subsequent trials of an SSRI and an SNRI were associated with symptom worsening, and nonpharmacologic interventions including CBT and TMS were also associated with symptom worsening. Between 07/2023–10/2023, he participated in a partial hospitalization program followed by step-down outpatient programming; the goal was management of anxiety as the primary working diagnosis at that time. Symptoms did not improve. Pharmacogenomic testing (GeneSight®) was obtained to guide medication selection; a subsequent desvenlafaxine trial was poorly tolerated.

The patient underwent neuropsychiatric gene-expression biomarker testing in 01/2024 (MindX One™ Blood Test, MindX Sciences) and a blood-based immune/inflammatory biomarker assay discussed later (ITI-PES™, Neo7 Biosciences; report dated 09/10/2025). NR3C1, GLUD1, and TREM2 were flagged in both reports despite different analytical platforms and scoring methodologies. NR3C1 encodes the glucocorticoid receptor, GLUD1 encodes mitochondrial glutamate dehydrogenase, and TREM2 encodes an innate immune receptor expressed on myeloid lineage cells. The recurrence of these genes across two independent assays indicates overlap at the level of reported biomarker outputs.

MindX One™ gene-expression biomarker testing (01/30/2024) flagged a set of genes whose established functions span broad groupings including immune-associated proteins, mitochondrial/metabolic proteins, transcription/chromatin regulators, cytoskeletal and neuron-associated proteins, vesicle/endosomal trafficking proteins, and cellular stress-response/protein homeostasis proteins.

Infectious Disease

Serologic reactivity to select tick-borne pathogens was identified on IGeneX testing (05/07/2025); however, subsequent PCR assays for *Babesia* and *Bartonella* were negative (08/15/2025). These findings were interpreted cautiously as serologic reactivity rather than evidence of tick-borne infection. IgeneX Lyme Panel, AcuDart, and Lyme PCR testing were non-reactive.

Vascular Medicine

On May 9, 2024, duplex venous ultrasound of the left lower extremity demonstrated mild venous reflux (>500 ms) in the left common femoral, femoral, and great saphenous veins with associated varicosities originating from the great saphenous vein, and no evidence of acute or chronic DVT. Autonomic dysfunction and systemic inflammation could contribute to venous pooling and symptom burden; however, the duplex study documents venous reflux as the primary abnormality.

Scope of Diagnostic Evaluation

Over the course of his illness, the patient underwent an extensive and repeated diagnostic evaluation across specialties. This included more than 40 emergency department visits and over 200 outpatient encounters across multiple specialties. These figures underestimate the total scope of care, as general practice visits, physical therapy, and other supportive care encounters were not included in these counts. While the volume of encounters may appear excessive, this does not capture the frequency or severity of symptoms nor the numerous instances in which the patient elected not to seek care due to repeated nondiagnostic evaluations and perceived lack of benefit. Visit totals by specialty are listed in parentheses.

Specialty care included cardiology (40+), emergency (40+), pulmonology (14), neurology (16), gastroenterology (24), hepatology (2), immunology (5), rheumatology (2), infectious disease (2), endocrinology (4), hematology (7), otolaryngology (19), ophthalmology (12), psychiatry (24), orthopedic medicine/physical medicine and rehabilitation (20+), urology (4), nephrology (3), bariatric medicine (1), multispecialty/general surgery (2), and vascular medicine (2).

Laboratory and Imaging Evaluation

Conservatively, this included over 100 non-routine laboratory investigations spanning autoimmune/rheumatologic (28), infectious disease (22), endocrine/metabolic (18), hematologic/coagulation (10), genetic (6), and multiple gastrointestinal and inflammatory testing categories. Longitudinal testing across institutions was performed to assess persistence, progression, or resolution of findings; repeat assays were not counted as separate investigations. The only consistently abnormal lab tests were low anion gap, and low free testosterone with normal total testosterone (Sex hormone binding globulin was normal).

In parallel, the patient underwent more than 100 imaging and functional diagnostic studies across cardiovascular, pulmonary, neurologic, ophthalmic, endocrine, gastrointestinal, musculoskeletal, and vascular systems. This included serial computed tomography of the head, chest, and abdomen; Doppler and other ultrasound studies; cardiac and non-cardiac magnetic resonance imaging; transthoracic and stress echocardiography; ambulatory rhythm monitoring; ventilation–perfusion scanning; pulmonary function testing; fluoroscopic and motility studies; endoscopic imaging; coronary calcium scoring and nuclear-based functional assessments; and repeated radiographic evaluations.

Across the course of evaluation, alternative etiologic mechanisms were systematically assessed and excluded across infectious, autoimmune, rheumatologic, genetic, hematologic, endocrine, malignant, toxic/medication-related, cardiovascular/vascular, metabolic, and primary neurologic domains. This comprehensive differential diagnostic process provides a rigorous framework for interpretation of the findings presented in this report.

Nucleocapsid Antibody Status and Spike Antibody Persistence

Following the myocarditis diagnosis, the evaluation shifted toward a unifying etiology; one focus was assessment for prior SARS-CoV-2 infection and consideration of myocarditis in the setting of Long COVID. The patient has no documented history of SARS-CoV-2 infection and remained nucleocapsid antibody negative through September 2025. Assessment of prior SARS-CoV-2 infection and humoral immune response was performed using serial nucleocapsid and spike antibody testing across multiple laboratories and time points. On May 8, 2024, 809 days following the patient's last COVID-19 vaccination, nucleocapsid antibodies were negative, while spike antibodies were reported as greater than the assay's upper reporting limit (>250 U/mL). The patient sought additional testing to better quantify spike antibody levels and to confirm the initial nucleocapsid result.

On June 13, 2024 (845 days post-vaccination), repeat testing demonstrated negative nucleocapsid antibodies with elevated spike antibody levels measuring 5,579 U/mL. Nucleocapsid antibodies again remained negative, with elevated spike antibody levels measuring 5,136 U/mL on December 23, 2024 (1,038 days post-vaccination). On September 25, 2025 (1,314 days post-vaccination), nucleocapsid antibodies remained negative at Labcorp, while spike antibody levels persisted at 4,130 U/mL. The most recent antibody test on January 23, 2026 (1,433 days post-vaccination) again demonstrated negative nucleocapsid antibodies, with persistently elevated spike antibody levels measuring 4,553 U/mL.

Across these serial measurements, nucleocapsid antibodies were undetectable at five separate time points spanning 809–1,433 days post-vaccination across three independent laboratories, while spike antibody levels remained persistently elevated more than three years after the patient's final COVID-19 vaccination, in the absence of serologic evidence of prior SARS-CoV-2 infection. Interpretation of SARS-CoV-2 nucleocapsid and spike antibody results was based on CDC antibody testing guidance. [10]

Cytokine Abnormalities and S1 Trafficking

On June 20, 2024 (852 days post-vaccination), Radiance Diagnostics (CLIA-certified), using the IncellDx Long Hauler Cytokine-14 Panel and COVID-19 S1 Immune Subset Panel, identified spike protein positive monocytes, including elevated CD14LO, CD16+S1

positive nonclassical monocytes at 3.36 (reference range: 0.00) and CD14++, CD16-+S1 positive classical monocytes at 0.77 (reference range: 0.00), demonstrating abnormal spike protein expression across multiple monocyte subsets. Concurrent cytokine profiling revealed immune signaling abnormalities, with elevations in interleukin-4 (IL-4) at 14.2 (reference range: 2.3–6.2), interleukin-13 (IL-13) at 13.7 (reference range: 1.5–6.1), interleukin-10 (IL-10) at 4.5 (reference range: 0.7–1.2), interferon-gamma (IFN-γ) at 27.8 (reference range: 1.8–3.5), and vascular endothelial growth factor (VEGF) at 14.2 (reference range: 2.0–12.3). The composite Long Hauler Index was elevated at 1.96 (reference range: ≤0.70). Additional abnormalities included reduced granulocyte-macrophage colony-stimulating factor (GM-CSF) at 3.6 (reference range: 5.8–77.0) and reduced CCL3 (MIP-1α) at 2.2 (reference range: 3.5–33.0), while tumor necrosis factor-alpha (TNF-α) and soluble CD40 ligand (sCD40L) remained within reference ranges.

Testing on December 5, 2024 (1,038 days post-vaccination) showed continued elevation of cytokines including IFN-γ (17.0), IL-10 (3.3), IL-13 (12.1), and IL-4 (15.6), improvement of the Long Hauler Index (0.25), absence of detectable S1-positive monocytes across subsets, and normalization of VEGF (10.6). Several immune markers remained suppressed or low, including GM-CSF (2.4), CCL3 (MIP-1α) (2.2), interleukin-6 (IL-6) (0.5), and interleukin-8 (IL-8) (3.3). Despite improvement in select markers, longitudinal testing continued to demonstrate persistent immune abnormalities across cytokine and cellular domains, consistent with immune dysregulation.

Recent testing on November 12th, 2025 (1,362 days post-vaccination) found reduced levels of IL-2 (1.1 pg/mL; reference 1.6–7.0), IL-6 (1.2 pg/mL; reference 1.4–3.0), IL-8 (3.3 pg/mL; reference 5.4–21.0), GM-CSF (3.6 pg/mL; reference 5.8–77.0), CCL3 (MIP-1α) (2.2 pg/mL; reference 3.5–33.0), and TNF-α (1.2 pg/mL; reference 3.7–11.0), alongside elevations in IL-4 (24.9 pg/mL; reference 2.3–6.2), IL-10 (2.7 pg/mL; reference 0.7–1.2), IL-13 (9.2 pg/mL; reference 1.5–6.1), IFN-γ (15.0 pg/mL; reference 1.8–3.5), VEGF (15.4 pg/mL; reference 2.0–12.3), and CCL5 (RANTES) (12,361.3 pg/mL; reference 7.2–11,800), with an elevated Long Hauler Index of 1.10 (reference ≤0.70), suggesting a persistent bidirectional pattern of immune dysregulation rather than uniform hyperinflammation.

Persistent Circulating Spike Protein and Spike-Specific IgG4 Antibodies

Two blood samples obtained at 1,173 and 1,284 days post-vaccination after the patient's final Pfizer-BioNTech COVID-19 mRNA vaccination demonstrated persistent abnormalities in spike antigen and antibody profiles (**Figure 5, panel a**). Quantitative ELISA identified free SARS-CoV-2 spike protein in plasma at 129.0 ± 4.1 fg/mL at 1,173 days post-vaccination, accompanied by markedly elevated spike-specific IgG4 (354.4 ± 22.4 ng/mL). Spike protein was simultaneously detectable in plasma-derived exosomes (11.6 ± 0.1 fg/mL) at this timepoint. By 1,284 days post-vaccination, spike protein was no longer detectable in either plasma or exosomes; however, IgG4 remained prominently elevated at 320.2 ± 4.4 ng/mL, suggesting ongoing antigenic stimulation even after antigen levels fell below the assay detection threshold. Spike protein was not detected in PBMC protein lysates at either timepoint.

Detection of Pfizer–BioNTech COVID-19 mRNA in Circulating Exosomes

To determine whether spike protein persistence could be attributed to ongoing expression from residual vaccine-derived mRNA, RT-PCR was performed on exosomal and PBMC RNA isolated at 1,284 days post-vaccination. Across three independent amplicons targeting the Pfizer/Moderna spike ORF (S1, S2, S3), exosomes demonstrated clear and reproducible amplification of vaccine mRNA sequences, with bands of the expected molecular weights on agarose gel electrophoresis (**Figure 5, panel b**). These findings provide direct molecular evidence that vaccine-derived mRNA persists within circulating exosomes more than 1,284 days after Pfizer–BioNTech COVID-19 mRNA vaccine administration.

In contrast, PBMC-derived RNA showed no detectable spike mRNA, suggesting that the long-term post-administration reservoir of vaccine mRNA is not intracellular within circulating leukocytes but instead localized to extracellular vesicular compartments. Given the established capacity of exosomes to deliver functional RNA cargo to recipient cells, these data identify a biologically plausible vehicle for prolonged, intermittent spike protein production.

Persistence of Pfizer–BioNTech COVID-19 Vaccine Plasmid DNA in PBMCs

Parallel PCR analyses targeting plasmid DNA elements used in Pfizer-BioNTech mRNA vaccine manufacturing revealed long-term persistence of replication-origin sequences—but not spike DNA or SV40 enhancer sequences—in PBMCs (**Figure 5, panels c-d**). Cytosolic plasmid DNA isolated from PBMCs at 1,284 days post-vaccination demonstrated distinct amplification of the origin-of-replication elements (ori1 and ori2), while PCR assays for spike DNA (S1–S3) and the SV40 enhancer were negative in all PBMC fractions.

The ori band was excised and confirmed by Sanger sequencing, validating that the detected DNA fragment corresponds precisely to the Pfizer–BioNTech COVID-19 mRNA vaccine plasmid backbone replication-origin region. No other plasmid components were

confirmed or detected in PBMCs. Exosomes yielded only faint or absent signals across all plasmid DNA targets, consistent with minimal or no plasmid DNA export into extracellular vesicles.

Together, these findings demonstrate persistent detection of replication-origin DNA sequences within PBMCs 1,284 days after vaccination; however, the biological source of this signal cannot be definitively assigned. While the ori fragment matches the Pfizer–BioNTech COVID-19 mRNA vaccine plasmid backbone by sequence, PBMCs are capable of internalizing and processing extracellular DNA, including bacterial DNA containing homologous replication-origin motifs. Accordingly, the ori signal may reflect intracellular uptake of replication-origin–like DNA fragments rather than intact vaccine plasmid persistence.

a

		plasma	exosomes	PBMC
M1	spike protein	129.0 ± 4.1 fg/ml	11.6 ± 0.1 fg/ml	n.d.
	spike IgG4	354.4 ± 22.4 ng/ml	n.a.	n.a.
M2	spike protein	n.d.	n.d.	n.d.
	spike IgG4	320.2 ± 44.1 ng/ml	n.a.	n.a.

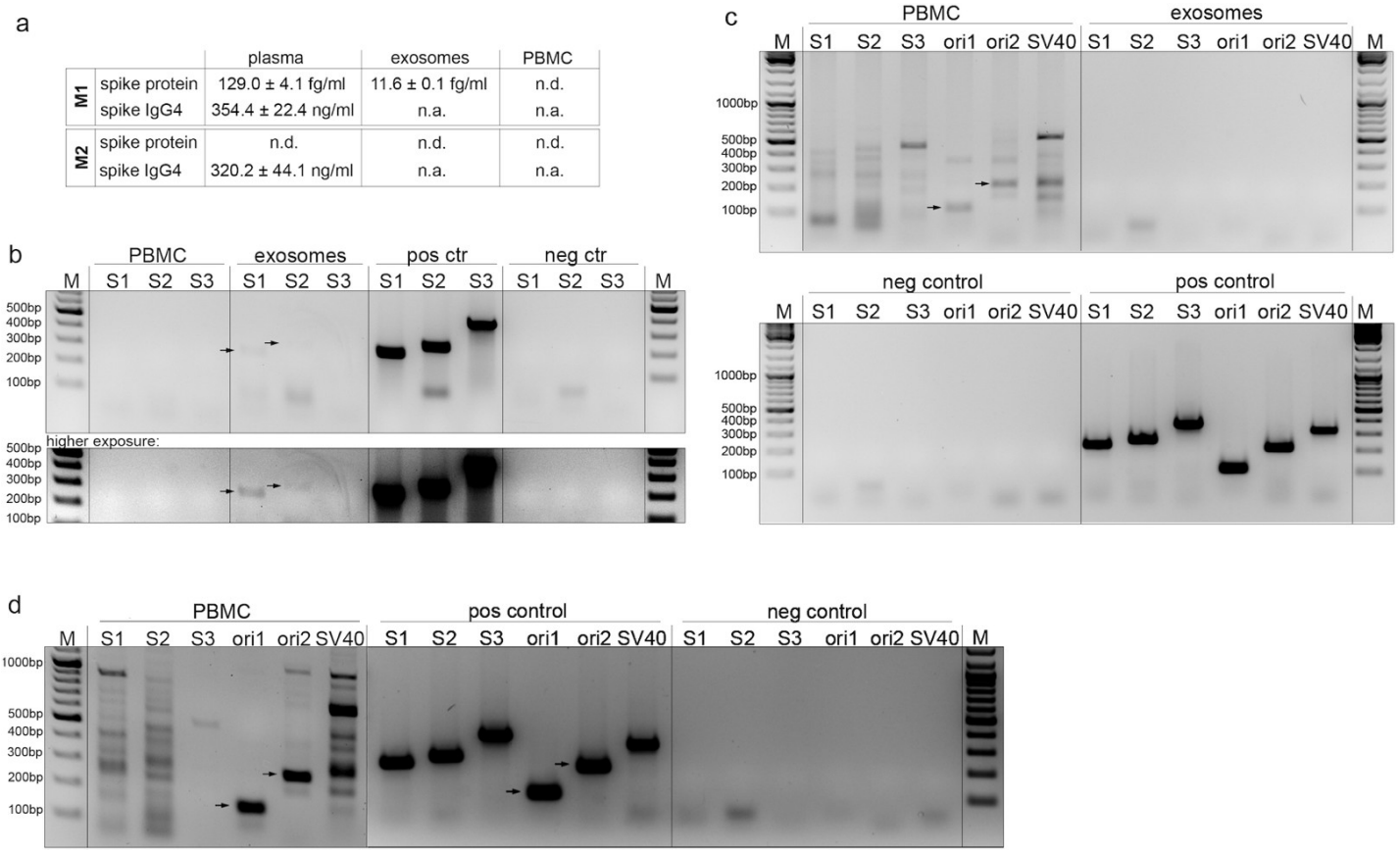

Figure 5. Molecular Detection of Spike Protein, Vaccine mRNA, and Plasmid DNA Elements in Peripheral Blood at 1,173-1,284 days Post-Vaccination

a. Levels of spike protein and IgG4 antibodies against spike protein in plasma, exosomes and PBMC prepared from EDTA blood samples were measured by quantitative ELISA. Measurement 1 was collected after 1,173 days after the last vaccination. Measurement 2 was a few months later (1,284 days post-vaccination). Data are given as mean ± standard of the mean. n.d., not detected; n.a. not applied; IgG4, immunoglobulin G4.

b. Qualitative detection of three independent spike protein sequences (S1-S3) of the vaccine mRNA by RT-PCR and agarose gel electrophoresis of the isolated total RNA obtained from PBMC and exosomes of EDTA blood samples taken 1,284 days after the last vaccination. Loading for cDNA: 9ng (PBMC) and 17ng (exosomes). The arrows indicate that the bands are positive for the respective DNA sequence.

c-d. Qualitative detection of different sequences for spike protein, ori and SV40 enhancer of cytosolic vaccine plasmid DNA residues **(c)** or total cellular DNA **(d)** after agarose gel electrophoresis in PBMC and exosomes obtained from EDTA blood samples taken 1,284 days after the last vaccination. Loading: 113ng plasmid DNA (PBMC) and 125ng total DNA (PBMC) and 1ng plasmid DNA (exosomes). Almost no plasmid DNA could be isolated from exosomes. The arrows mark the bands that represent the origin of replication sequence, whose DNA was cut from the gel, purified, and confirmed by Sanger sequencing.

M1, measurement 1; M2, measurement 2; S, spike protein; ori, origin of replication; SV40, SV40 enhancer sequence; bp, base pairs; M, marker; pos ctr, positive control (vaccine vial); neg ctr, negative control (non template control); PBMC, peripheral blood mononuclear cells.

Persistent Pfizer–BioNTech COVID-19 Vaccine Plasmid DNA in Somatic Tissue

A skin biopsy obtained 1,364 days post-vaccination from an area clinically affected by Grover's disease was subjected to RNA and DNA analysis. RT-PCR of tissue RNA revealed no detectable spike mRNA, confirming that vaccine-derived transcripts were not present or were below detection levels within this somatic sample (**Figure 6, panel a**).

In contrast, PCR performed on genomic DNA extracted from the same biopsy demonstrated clear detection of spike DNA sequences (S1–S3), both origins of replication, and the SV40 enhancer, consistent with durable retention of vaccine plasmid DNA within non-immune, somatic tissue (**Figure 6, panel b**). The patient denies known SV40 exposure through recognized historical or occupational routes, including SV40-contaminated early polio vaccination (1955–1963), laboratory or primate contact, or documented secondary transmission. SV40-derived regulatory sequence elements have been used in plasmid DNA constructs associated with the manufacturing template for Pfizer–BioNTech COVID-19 mRNA vaccine (BNT162b2). These results provide direct molecular evidence that vaccine- derived plasmid sequences localized to subcutaneous tissue and remained detectable more than 1,364 days after vaccination.

Histopathological and Immunohistochemical Evidence of Chronic Spike Protein Deposition

Histological examination of serial skin biopsies collected at 1,160, 1,249, and 1,364 days post-vaccination (all obtained from truncal skin within areas of clinically active Grover's disease lesions) revealed persistent and evolving inflammatory changes. At 1,160 days post-vaccination, tissue demonstrated mild solar elastosis with discrete perivascular inflammatory infiltrates (**Figure 6, panel c**). Immunohistochemistry identified SARS-CoV-2 spike subunit 1 protein within endothelial cells and perivascular macrophages, whereas nucleocapsid protein was absent (**Figure 6, panel d**), excluding prior SARS-CoV-2 infection as the source of antigen.

At 1,249 days post-vaccination, the dermis featured a mixture of vascular connective tissue and adipose structures with sparse epidermal remnants (**Figure 6, panel e**). Spike protein remained detectable within scattered perivascular macrophages (**Figure 6, panel f**). By 1,364 days post-vaccination, the biopsy demonstrated moderate to pronounced perivascular, periadnexal, and perineural inflammatory infiltration, composed of lymphocytes, macrophages, mast cells, and eosinophils (**Figure 6, panel g**). Immunohistochemistry again identified persistent spike protein deposition, including expression in nerve fibers and perivascular macrophages, with continued absence of nucleocapsid staining (**Figure 6, panel h**).

These findings document chronic, multi-site accumulation of spike protein in endothelial, macrophage, and neural compartments extending over 1,364 days after vaccination, with no evidence that the antigen originated from infection. **Table 1** provides an integrated summary of these longitudinal results.

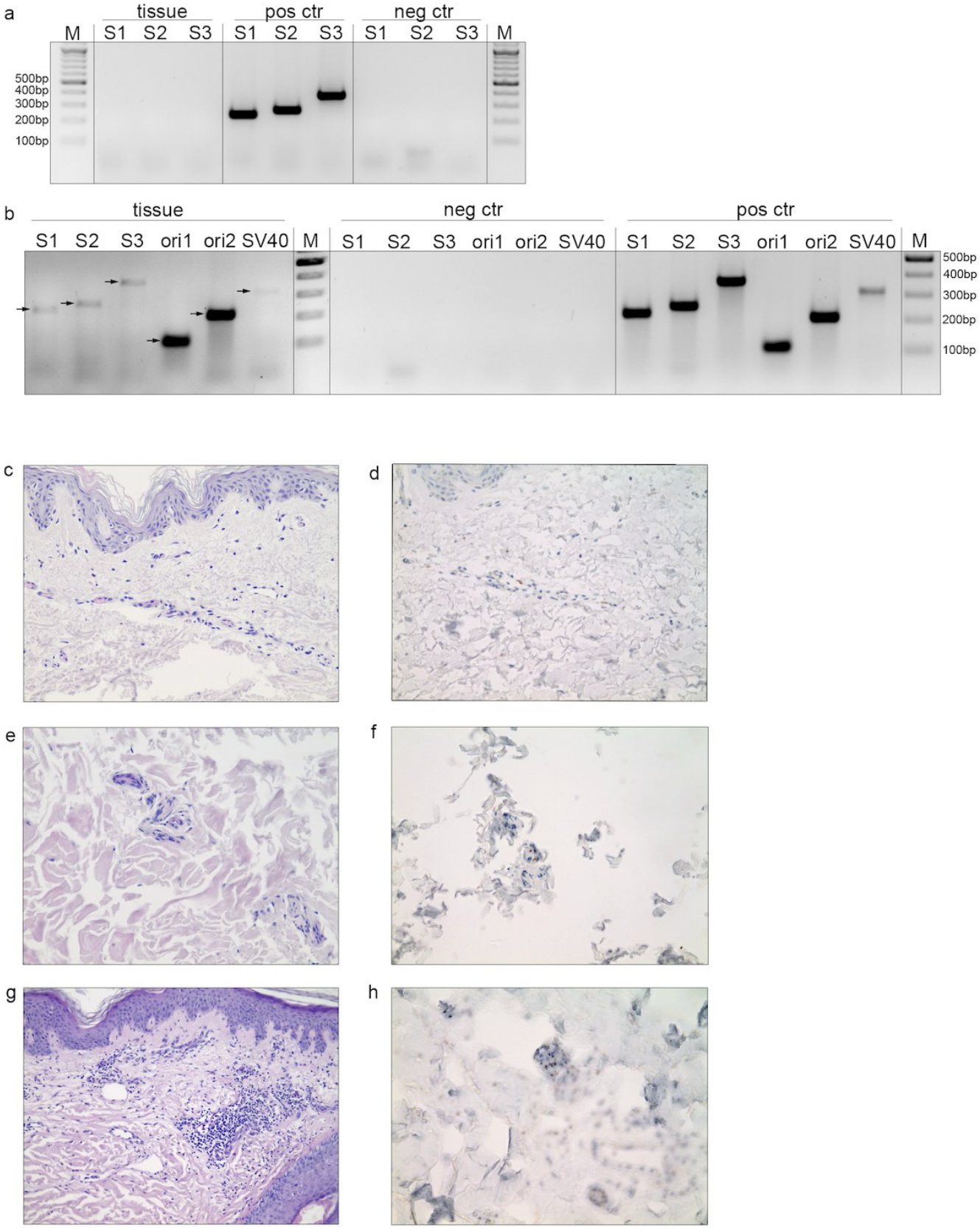

Figure 6. Detection of Vaccine-Derived DNA and Histopathologic Evidence of Persistent Spike Protein in Serial Truncal Skin Biopsies Obtained from Areas of Clinically Active Grover's Disease (1,160 to 1,364 Days Post-Vaccination).

a. Qualitative detection of three independent spike protein sequences (S1-S3) of the vaccine mRNA by RT-PCR and agarose gel electrophoresis of the isolated total RNA obtained from skin biopsy taken 1,364 days after the last vaccination. Loading for cDNA: 14ng. No spike protein mRNA is detectable in the tissue.

b. Qualitative detection of different sequences for spike protein, ori and SV40 enhancer of total cellular DNA after agarose gel electrophoresis in skin biopsy taken 1,364 days after the last vaccination. Loading: 79ng DNA. The arrows indicate the bands that represent the different plasmid sequences.

S, spike protein; ori, origin of replication; SV40, SV40 enhancer sequence; bp, base pairs; M, marker; pos ctr, positive control (vaccine vial); neg ctr, negative control (non template control).

c–h. All tissue biopsies were obtained from truncal skin within areas of clinically active Grover's disease lesions.

c-d. Skin tissue from 1,160 days after the last vaccination. **(c)** Tissue shows minor sun damage and discrete perivascular inflammatory infiltration in the upper dermis. H&E stain, 200x magnification. **(d)** SARS-CoV-2 spike subunit 1 detected in endothelial cells and perivascular macrophages. No SARS-CoV-2 nucleocapsid detected (not shown). Immunohistochemistry, spike protein in brown, 200x magnification.

e-f. Skin tissue from 1,249 days after the last vaccination. **(e)** Tissue shows vascular connective and adipose tissue with only sparse epidermal layers remaining. Moderate sun damage is present. H&E stain, 200x magnification. **(f)** SARS-CoV-2 spike subunit 1 is detected in individual perivascular macrophages. SARS-CoV-2 nucleocapsid is not detected (not shown). Immunohistochemistry, spike protein in brown, 200x magnification.

g-h. Skin tissue from 1,364 days after the last vaccination. **(g)** Skin biopsy shows mildly hyperkeratotic epidermis, moderate sun damage, and a moderate to pronounced perivascular, periadnexal, and perineural inflammatory infiltrate. This infiltrate consists of lymphocytes, macrophages, mast cells, and eosinophilic granulocytes. H&E stain, 200x magnification. **(h)** SARS-CoV-2 spike subunit 1 was detected in individual perivascular macrophages and in some nerve fibers. SARS-CoV-2 nucleocapsid is not detected (not shown). Immunohistochemistry, spike protein in brown, 200x magnification.

Sample Date	Days Since Last Vaccine	Test / Event	Key Findings
02/20/2022	N/A	Pfizer mRNA COVID-19 vaccine – Booster	Booster dose administered
05/08/2024	809 days	Nucleocapsid & Spike Antibodies	Nucleocapsid negative; spike antibody >250 (above assay upper reporting limit)
06/13/2024	845 days	Nucleocapsid & Spike Antibodies	Nucleocapsid negative; spike antibody 5,579 U/mL (elevated)
06/20/2024	852 days	IncellDx Long Hauler & COVID-19 S1 Immune Subset Panel	S1-positive monocytes detected (CD14loCD16+ nonclassical 3.36; CD14++CD16− classical 0.77); cytokine abnormalities; Long Hauler Index 1.96 (elevated)
12/05/2024	1,020 days	IncellDx Long Hauler & COVID-19 S1 Immune Subset Panel	Persistent cytokine abnormalities; S1-positive monocytes no longer detected
12/23/2024	1,038 days	Nucleocapsid & Spike Antibodies	Nucleocapsid negative; spike antibody 5,136 U/mL (elevated)
04/24/2025	1,160 days	Grover's lesion trunk biopsy (PCR + histology/IHC)	SARS-CoV-2 Spike S1 subunit positive in endothelial cells; Spike S1 subunit positive in perivascular macrophages; nucleocapsid not detected
05/07/2025	1,173 days	Plasma/PBMC testing	Spike proteins in plasma 129.01 +/- fg/mL; Spike proteins in exosomes 11.65 +/-; IgG4 spike protein Ab 354.4 +/-
07/22/2025	1,249 days	Grover's lesion trunk biopsy (histology/IHC)	SARS-CoV-2 Spike S1 subunit positive in perivascular macrophages; nucleocapsid not detected
08/19/2025	1,277 days	Multi-Omic Analysis	Structural genomic instability, redox and mitochondrial stress, endothelial activation and a proteomic signature of chronic inflammation and vascular injury.
08/26/2025	1,284 days	Plasma/PBMC testing	Plasmid DNA in PBMC positive (ori 1, 2); vaccine mRNA in exosomes positive (S1 and S2 SPIKE sequence); IgG4 spike protein Ab 320.2 +/-
09/17/2025	1,306 days	Urine Proteomic Analysis	Systemic inflammatory proteomic signature consistent with immune activation and vascular leakage (non-renal)
09/25/2025	1,314 days	Nucleocapsid & Spike Antibodies	Nucleocapsid negative; spike antibody 4,130 U/mL (elevated)
11/12/2025	1,362 days	IncellDx Long Hauler & COVID-19 S1 Immune Subset Panel	Persistent cytokine abnormalities; VEGF increased; Long Hauler Index 1.10 (elevated)
11/14/2025	1,364 days	Grover's lesion trunk biopsy (PCR + histology/IHC)	Vaccine plasmid DNA positive (SV40, ori 1, ori 2: all positive); vaccine plasmid DNA fragments positive (sequence 1; sequence 2; sequence 3); SARS-CoV-2 Spike S1 subunit positive in nerve fibers; Spike S1 subunit positive in endothelial cells; Spike S1 subunit positive in perivascular macrophages; nucleocapsid not detected
01/23/2026	1,433 days	Nucleocapsid & Spike Antibodies	Nucleocapsid negative; spike antibody 4,553 U/mL (elevated)

Table 1. Integrated Laboratory Findings Timeline. Testing across multiple time points identified spike-related findings and vaccine-specific components in blood and tissue (including plasma, exosome, and PBMC assays, as well as tissue immunohistochemistry), with concordant detection by multiple independent laboratories (Inmodia and Radiance). Nucleocapsid antibodies were repeatedly negative across five separate tests from three independent laboratories, and nucleocapsid protein was not detected in three skin biopsies that demonstrated spike S1 subunit deposition.

Multi-Omic Analysis

On August 19, 2025, 1,277 days post-vaccination, whole-blood genomic DNA was collected, and structural variant (SV) analysis identified 27,172 candidate events, including broad copy-number–like alterations and complex rearrangements consistent with genomic instability. A large duplication on chromosome 7p (~35.9–56.3 Mb) encompassed the EGFR locus (SU ≈ 11). Additional multi-megabase duplications and deletions were observed in regions containing MYC (8q24), ERBB2/HER2 (17q12), and ETV6/RUNX1 (12p13/21q22). A localized small deletion near EGFR (chr7:55.219–55.214 Mb) further indicated instability in this region. In addition, comparison of RNA-seq with matched whole-genome sequencing (WGS) revealed RNA-only coding variants in translation/ribosome (EIF2A, EIF3A, EIF5, RPS14, NOP56, RRP9, RRP12, FBL), mRNA surveillance/NMD (UPF1, UPF2, SMG1), small-RNA processing (DICER1, AGO2, DGCR8), epigenetic regulation (CHD4, HDAC1, DNMT1), and TP53.

Whole-blood transcriptomics were analyzed by REViSS/aHI-PBIMA, which demonstrated marked dysregulation of genes aligned with the patient's symptom domains: GPX4 was downregulated (−2.2), indicating impaired redox control and mitochondrial stress; ACE was upregulated (+4.6), consistent with endothelial activation and RAAS imbalance; APC was markedly reduced (−6.1), aligning with gastrointestinal barrier disruption and dysbiosis; and LMNA was decreased (−3.7), suggesting nuclear structural stress relevant to cardiomyocyte and neuronal vulnerability. Hallmark scoring showed a predominance of unfavorable signals in vascular, mitochondrial, and gastrointestinal axes, concordant with the patient's myocarditis, prior pulmonary emboli, chronic fatigue with

dysautonomia, dermatologic inflammation, and intestinal symptoms. These transcriptomic findings corroborate the contemporaneous proteomic evidence of systemic inflammation and support a persistent spike- associated inflammatory state.

Urine for a comprehensive proteomic analysis was collected on September 17, 2025, to evaluate systemic protein excretion patterns reflective of persistent inflammation and immune activation. Quantitative mass spectrometry identified marked elevation of proteins linked to innate immune signaling (S100A8, S100A9, CAMP), complement and acute-phase response (C3, CFH, SERPINA1), oxidative stress and endothelial injury (PRDX1, APOE, HP, HPX), and adaptive antibody regulation (IGHG1–4, IGHA1, B2M). These proteins, typically undetectable or present only in trace amounts in healthy urine, indicate systemic overproduction and inflammation-driven vascular leakage rather than primary renal dysfunction. Full proteomic datasets are presented in **Supplemental Tables S1–S4**.

Genetic testing identified the presence of HLA-B*07:02 and HLA-DRB1*11:04, both alleles associated with heightened immune reactivity [11]. HLA-B*07:02, a class I allele, is known to influence $CD8^+$ T-cell responses to viral antigens strongly and can present peptides through both conventional and alternative antigen-processing pathways, potentially sustaining antigen presentation[12]. HLA-DRB1*11:04, a class II allele, has been linked to increased immune sensitivity and a propensity for inflammatory and autoimmune responses[13]. The coexistence of these alleles may contribute to the patient's chronic inflammatory profile and prolonged immune activation observed post-vaccination[14].

Targeted Treatment of Spike-Associated Pathology

The principal treatments have included maraviroc and atorvastatin (August 2024–March 2025) [7]; the McCullough protocol "Base Spike Detoxification" regimen (March 2025–ongoing) [15]; colchicine; apixaban; and supplemental nutraceuticals. Following maraviroc and atorvastatin, the patient demonstrated a decreased Radiance Diagnostics Long Hauler Index, improved VEGF, and no longer had detectable S1 in monocytes. Since initiating the McCullough "Base Spike Detoxification" regimen, spike antibody levels have declined, and spike is no longer detected in plasma. Despite these improvements, the patient remains symptomatic. The patient began long-term disability in June 2023 and remains unable to work.

Although circulating spike protein and S1-positive monocytes were no longer detected following treatment, spike-specific antibodies remain persistently elevated. Markers of genomic instability and persistent detection of spike protein, mRNA, plasmid DNA, and cytokine abnormalities also remain, and the patient remains symptomatic. These observations reflect a single-patient response, and controlled studies are required to define the clinical relevance of persistent vaccine-derived components and to determine whether targeted interventions can safely and reproducibly modify these processes. Both total anti-spike antibodies and the IgG4 subclass can bind spike protein and form immune complexes that may not be detected by conventional free-antigen assays. This phenomenon of immune-complex sequestration and epitope masking may lead to underestimation of total antigen burden and should be considered when interpreting low or undetectable spike protein results in the setting of persistently elevated spike antibody titers.

Discussion

After more than 100 non-routine laboratory investigations, over 100 imaging and functional studies, and systematic exclusion of a broad spectrum of alternative etiologic mechanisms across multiple clinical domains, this case demonstrates persistent detection of spike protein and mRNA vaccine–related nucleic acid sequences extending to 3.7 years after the patient's final Pfizer–BioNTech COVID-19 mRNA vaccination. Serial serologic assessments spanning 809–1,433 days post-vaccination showed five nucleocapsid antibody–negative results across three independent laboratories, and nucleocapsid protein was absent in all spike-positive tissue specimens, effectively ruling out prior SARS-CoV-2 infection as the source of the detected spike protein and genetic material. The vaccine- and spike-related findings were generated across multiple independent laboratories at multiple time points using orthogonal analytical methodologies—including high-sensitivity ELISA, automated immunohistochemistry with histopathologic correlation, RT-PCR, standard PCR with Sanger sequencing confirmation, whole-genome sequencing, transcriptomic profiling, and quantitative mass spectrometry—in distinct biospecimens comprising plasma, circulating exosomes, peripheral blood mononuclear cells, urine, and serial truncal skin biopsies. Convergent detection of spike protein, spike mRNA sequences, and plasmid backbone DNA elements across independent platforms and biological compartments supports the reproducibility and internal consistency of these observations. These findings describe a degree of long-term molecular persistence not previously reported in humans following mRNA vaccination. Spike protein remained detectable in plasma and exosomes at 1,173 days post-vaccination, and immunohistochemistry confirmed its continued presence within endothelial cells, perivascular macrophages, and nerve fibers in serial skin biopsies up to 1,364 days after vaccination. The detection of spike protein within exosomes is particularly significant, as exosomal loading is an active and regulated

cellular process, indicating ongoing intracellular handling or production of spike protein, rather than passive circulation of residual antigen. In parallel, vaccine-derived mRNA— long assumed to degrade within hours to days—was clearly amplified from circulating exosomes at 1,284 days after vaccination, marking the longest known in vivo persistence of mRNA from any therapeutic or vaccine platform. Because exosomes selectively package RNA through defined cellular pathways, the presence of intact spike mRNA in this compartment suggests a biologically active reservoir capable of enabling prolonged, intermittent spike protein expression. At the DNA level, replication-origin sequences (ori1 and ori2) from the Pfizer–BioNTech COVID-19 mRNA vaccine plasmid backbone were detected within PBMCs at 1,284 days post-vaccination, while spike DNA and SV40 enhancer sequences were absent in the blood compartment. However, because PBMCs routinely internalize and process extracellular nucleic acids, including bacterial DNA containing homologous replication-origin motifs, the detected ori signal may reflect uptake of replication-origin–like DNA fragments rather than intact or functional vaccine plasmid persistence. In contrast, the skin biopsy revealed a broader persistence of plasmid DNA elements, including spike gene fragments, ori1/ori2, and the SV40 enhancer. These findings directly demonstrate that vaccine-related genetic material can persist long-term in both immune and non-immune tissues, with different plasmid fragments surviving in different biological niches. DNA contamination in COVID-19 vaccines has previously been documented across multiple manufacturers, platforms, and countries—with measured levels exceeding regulatory thresholds by up to 65,500% [16].

Importantly, this molecular profile aligns with the patient's clinical course, which included pulmonary embolism, myocarditis confirmed by cardiac MRI despite normal troponin and natriuretic peptide levels, and a progressive constellation of multisystem symptoms consistent with post-vaccination syndrome. Persistent spike protein in circulation and within exosomes may contribute to continued endothelial activation, immune dysregulation, and microvascular injury—mechanisms implicated in thrombotic and cardiac complications following mRNA vaccination [2]. To contextualize the longitudinal molecular detections alongside the patient's confirmed multi-system clinical manifestations, **Figure 7** provides an integrated visual summary of persistent vaccine-derived biomaterials, genomic dysregulation, and organ-system involvement identified up to 3.7 years post-vaccination.

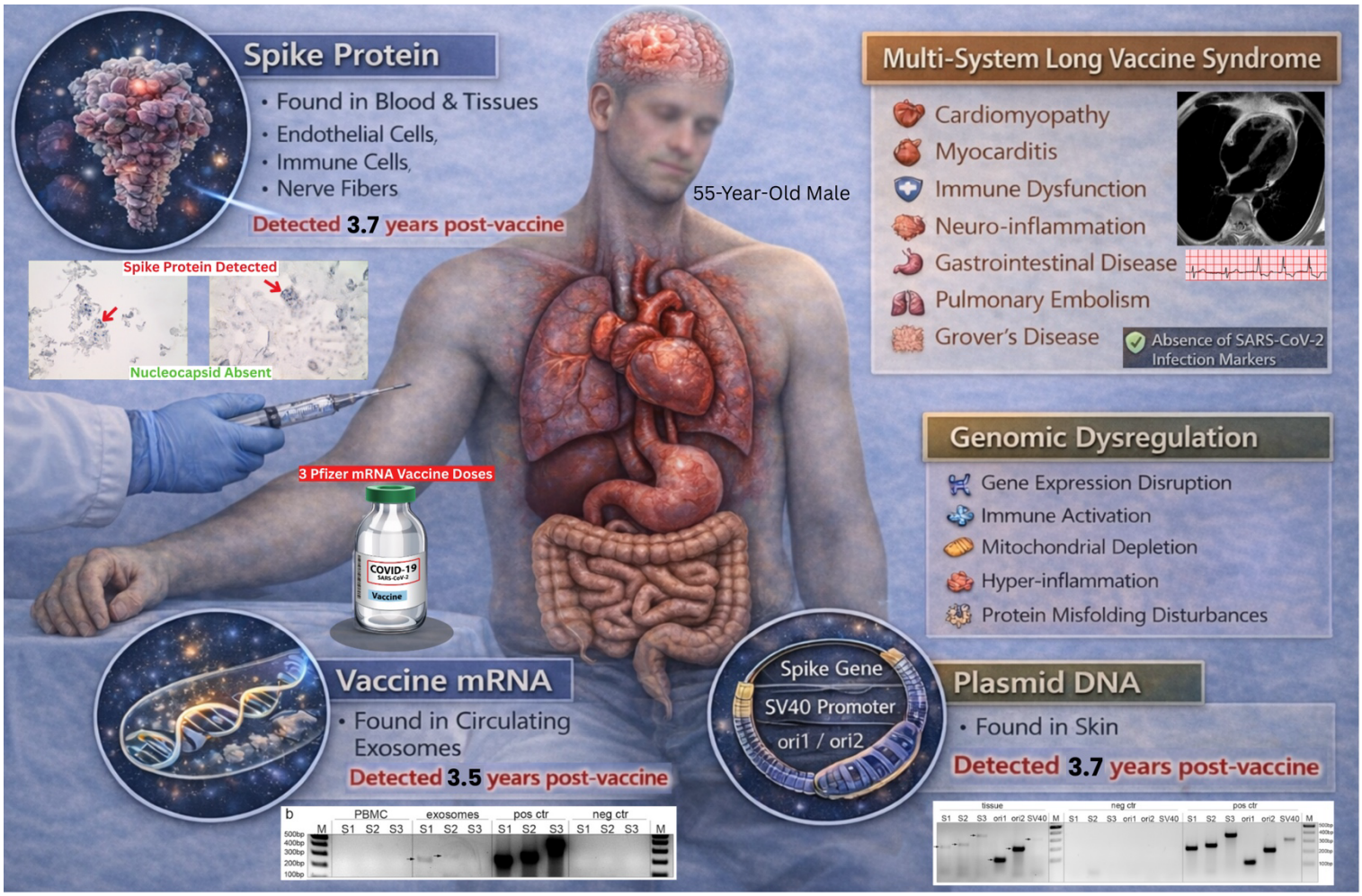

Figure 7. Integrated Molecular Persistence and Multi-System Clinical Findings 3.7 Years After COVID-19 mRNA Vaccination.

The combined presence of persistent plasmid DNA fragments, exosomal vaccine mRNA, and long-lived spike protein raises important mechanistic considerations. Although this case does not prove genomic integration, the extended presence of multiple mRNA vaccine components within host cells raises the possibility of extrachromosomal persistence or insertional events, especially given published evidence demonstrating reverse transcription and genomic incorporation of vaccine-related sequences in vitro [17, 18] and in vivo [19]. These findings underscore the urgent need for long-term molecular surveillance of individuals presenting with chronic symptoms following mRNA vaccination, and call for a reassessment of the assumptions surrounding the pharmacokinetics and biological fate of mRNA vaccine components.

In the Comirnaty European Public Assessment Report (EPAR; pp. 46–47), the EMA states that no traditional pharmacokinetic or biodistribution studies were performed with the vaccine candidate BNT162b2, and biodistribution was instead assessed in non-GLP rodent studies using surrogate reporter formulations [20]. The applicant evaluated a luciferase modRNA surrogate formulated in an LNP using in vivo bioluminescence (IVIS) in mice, and a radiolabeled ([^{3}H]) LNP–mRNA formulation in rats, which was described as more sensitive and demonstrated a broader biodistribution pattern. In mice (3 females per group), IVIS detected luciferase signal at the injection sites and in the liver region (interpreted as drainage to liver), with readouts extending to 9 days. In rats followed for 48 hours after a single 50 µg IM dose, radioactivity was detected in most tissues from the earliest timepoint, with the injection site and liver as major sites; outside the injection site, recovered signal was greatest in the liver (up to 21.5% of injected dose) and substantially lower in spleen, adrenal glands, and ovaries. Because radiolabeling is more sensitive, it is preferred for biodistribution and can detect low-level tissue distribution that reporter imaging may miss; accordingly, the mouse IVIS finding that liver-region signal returned to background by ~48 hours reflects loss of detectable luciferase expression rather than confirmed clearance of LNP-associated material. A key limitation is the short observation windows, 48 hours for radiolabeled biodistribution in rats and 9 days for IVIS reporter expression in mice, which characterize early distribution but do not establish longer-term clearance or persistence [20].

Given the widespread biodistribution of COVID-19 mRNA vaccines [2,4-6], it is unsurprising that patients with post-vaccination syndrome generally have an extremely varied and exhaustive list of symptoms creating diagnostic challenges for clinicians. Additionally, it can be difficult to delineate if symptoms are attributable to the virus or vaccine given that the vast majority of patients have had both previous infection as well as vaccination. The detection of plasma antibodies to the nucleocapsid protein of SARS-CoV-2 is the most sensitive test for previous infection [21]. The absence of the nucleocapsid antibody conveys a lack of immunity to the virus itself. Therefore, a patient who is positive for spike protein without the presence of nucleocapsid antibody, the spike is ascribed to vaccination rather than infection.

A thrombogenic effect of the SARS-CoV-2 virus was noted early in the pandemic cases of life- threatening thromboembolic disorders including pulmonary emboli [22]. These same conditions have been reported after COVID-19 vaccination, likely due to the thrombogenic nature of the spike protein [2,23]. Additionally, a causal link between COVID-19 vaccination and myocarditis has been firmly established [8,24]. In a multinational cohort study of over 99 million vaccinated individuals, Faksova et al identified a significant safety signal for myocarditis, with a reported 510% increase in risk following the second dose of COVID-19 mRNA vaccines [25]. Although cardiac risk from SARS-CoV-2 infection has been widely described, it has been established that there are substantially more cardiac risks post-vaccination [8]. Schauer et al found that although a rapid improvement of myopericarditis symptoms in adolescents was experienced after the second dose of Pfizer–BioNTech COVID-19 mRNA vaccine, 70% had persistent cardiac MRI changes at their 3-8 month follow up [26]. These structural changes may have long- term prognostic implications that remain poorly understood. A recently proposed risk stratification framework addresses the growing incidence of sudden cardiac arrest in previously healthy individuals post-vaccination by highlighting subclinical myocarditis as a likely mechanism—often undetectable on standard imaging or autopsy [27]. The approach emphasizes the use of antibody levels, cardiac biomarkers, and advanced imaging to identify high-risk individuals. Notably, our patient's case underscores its clinical relevance: despite normal biomarkers and cardiac stress testing, cardiac MRI confirmed active myocarditis—highlighting the limited sensitivity of routine diagnostics for detecting vaccine-associated cardiac injury in this patient.

The patient received three Pfizer-BioNTech COVID-19 mRNA vaccine doses, each traceable to specific lot numbers associated with documented severe adverse events. Using the VAERS- linked *How Bad Is My Batch* search tool [28], we identified significant numbers of reported cases of myocarditis, pulmonary embolism (PE), hospitalizations, and deaths for each lot:

1. **March 3, 2021 – Lot EN6202**: 11 myocarditis, 17 PE, 830 hospitalizations, 180 deaths
2. **March 24, 2021 – Lot ER8727**: 5 myocarditis, 13 PE, 463 hospitalizations, 97 deaths

3. **February 20, 2022 – Lot FK9894**: 3 myocarditis, 5 PE, 186 hospitalizations, 20 deaths

These data suggest non-random clustering of serious adverse event reports that warrants further formal pharmacovigilance analysis.

After suspecting a vaccine-related injury, the patient reported the case to the Vaccine Adverse Event Reporting System (VAERS). VAERS intake staff did not capture in detail the multi-system, longitudinal nature of the illness and instead emphasized identifying the hospital where a diagnosis occurred for follow-up. The patient reports being informed by VAERS staff and the Countermeasures Injury Compensation Program (CICP) that reporting and claim eligibility were limited to one year after vaccination. In this case, suspicion did not arise until more than two years post-vaccination, and assembling corroborating records required substantially longer. In this case, delayed recognition of a vaccine-associated, multisystem condition intersected with time-limited post-authorization reporting and compensation pathways, including VAERS reporting norms and the PREP Act–linked Countermeasures Injury Compensation Program (CICP). Because suspicion of a vaccine-related etiology emerged more than two years after vaccination, the patient's clinical timeline did not align with several time-dependent administrative processes despite persistent impairment. This timing mismatch may influence access to compensation mechanisms and employment-related benefit determinations, including workers' compensation, long-term disability, and supplemental critical illness coverage.

There has been considerable scientific discussion surrounding the persistence of SARS-CoV-2 spike protein in the body following mRNA vaccination. **Table 2** summarizes confirmed detections reported in the peer-reviewed literature. Estimates of spike protein duration vary widely. Brogna et al. detected recombinant vaccine spike protein fragments in blood samples up to 187 days post-vaccination, independent of antibody titers [29]. Patterson et al. identified the S1 subunit of spike protein in CD16+ monocytes up to 245 days in individuals with post-COVID-19 vaccine syndrome (PCVS) who tested negative for prior SARS-CoV-2 infection [7]. Ota et al. reported spike protein expression in the cerebral arteries up to 17 months after vaccination in hemorrhagic stroke patients, with absence of nucleocapsid protein confirming non-infectious origin [4]. Bhattacharjee et al. detected circulating spike protein in plasma up to 709 days after COVID-19 mRNA vaccination [30]. However, the present case represents the longest documented interval between COVID-19 mRNA vaccination and confirmed spike protein detection to date.

Study (Year)	Detection Site	Detection Method	Max Duration (Days)
Brogna et al. (2023) [29]	Plasma	Mass spectrometry (PP-Spike peptide fragments)	187
Patterson et al. (2025) [7]	$CD16^+$ monocytes	Flow cytometry + LC-MS (S1 subunit)	245
Ota et al. (2025) [4]	Cerebral arteries	Immunohistochemistry + in situ hybridization (spike mRNA)	518
Bhattacharjee et al. (2025) [30]	Plasma	SPEAR immunoassay (Successive Proximity Extension Amplification Reaction) detecting S1 and full-length spike	709

Table 2. Documented Persistence of Spike Protein Following COVID-19 mRNA Vaccination

Patients experiencing syndrome have lengthy convoluted medical histories involving many physicians and specialists that may or may not have a temporal correlation to the COVID-19 vaccine. Their symptoms may be described as relatively vague and disjointed, particularly early on. Patients may often be diagnosed with anxiety, depression, or another psychiatric condition in addition to numerous seemingly unconnected diagnoses. Post-vaccination syndromes can involve numerous organ systems, complicating diagnosis and treatment. There is a limited number of specialists with training to evaluate and manage multisystem presentations, which may restrict access to appropriate care. The extent of psychological stress experienced by patients navigating prolonged diagnostic uncertainty cannot be overstated.

Whole-genome structural variant analysis was completed using LUMPY, which identified 27,172 candidate events, revealing multiple broad copy-number–like alterations and complex rearrangements reminiscent of cancer-associated genomic instability. A large regional duplication spanning chromosome 7p (~35.9–56.3 Mb) encompassed the EGFR locus (SU ≈ 11), consistent with somatic

copy-number gains frequently observed in solid tumors. Additional multi-megabase interstitial duplications and deletions were observed in regions harboring MYC (8q24), ERBB2/HER2 (17q12), and ETV6/RUNX1 (12p13/21q22)—all canonical cancer-related loci. Although these broad events may represent tumor-type CNVs, germline CNVs, or mapping artifacts from single-sample analysis, their pattern of arm-level DUP/DEL and dense breakend (BND) distribution (~18k events) is strongly suggestive of chromosomal fragility and aberrant repair activity, consistent with oncogenic transformation. A moderate-confidence small deletion near the EGFR locus (chr7:55.219–55.214 Mb, SU = 47, SR = 31) further supports localized instability within this oncogenic region. Collectively, these findings demonstrate structural perturbations characteristic of tumorigenic genomes, though definitive oncogenic classification would require matched-normal comparison, depth-based CNV validation, and gene-level annotation. Given the single-sample limitation of the current dataset, duplicate sampling, orthogonal validation, and longitudinal re-analysis are warranted to confirm the reproducibility and biological relevance of these events. Within the context of persistent spike- associated transcriptomic dysregulation described in this case, these SV patterns support a mechanistic link between genomic instability, aberrant DNA repair, and oncogenic susceptibility following sustained post-vaccination molecular stress [31-34]. In addition, comparing RNA-seq with matched WGS identified RNA-only coding variants across core pathways— translation/ribosome (EIF2A, EIF3A, EIF5, RPS14, NOP56, RRP9, RRP12, FBL), mRNA surveillance/NMD (UPF1, UPF2, SMG1), small-RNA processing (DICER1, AGO2, DGCR8), epigenetic regulation (CHD4, HDAC1, DNMT1), and TP53. These genes were previously reported in our prior study [3]; therefore, the pathways they anchor warrant careful interrogation in this cohort. All sites were absent in matched DNA, indicating true RNA–DNA mismatches rather than uncalled germline variants.

Transcriptomic profiling further supported the patient's clinical presentation by revealing dysregulation of key genes associated with mitochondrial, vascular, intestinal, and structural integrity. Downregulation of GPX4, a key antioxidant enzyme, suggests impaired redox homeostasis and increased susceptibility to ferroptosis, consistent with mitochondrial oxidative stress observed in myocarditis and chronic fatigue. Upregulation of ACE indicates a renin– angiotensin system imbalance and endothelial injury, mechanisms that promote vascular inflammation and thrombosis, consistent with the diagnosis of pulmonary embolism. Reduced APC expression compromises intestinal epithelial integrity and immune regulation, aligning with the patient's dysbiosis and chronic inflammation. Finally, decreased LMNA, essential for nuclear stability in cardiomyocytes and neurons, may underlie persistent cardiac dysfunction and neurocognitive symptoms. Together, these transcriptomic abnormalities provide a molecular framework linking oxidative stress, endothelial activation, barrier disruption, and nuclear instability to the patient's post-mRNA vaccine multi-system pathology.

The urine proteomic analysis conducted on September 11, 2025, provides further molecular corroboration of persistent systemic inflammation and immune dysregulation in this patient. The analysis utilized both Direct and Extracellular Vesicle (EV) proteomic technologies, a dual approach that significantly enhances detection sensitivity compared to direct analysis alone.

Quantitative mass spectrometry revealed a distinct inflammatory proteomic signature characterized by upregulation of innate immune mediators (S100A8, S100A9, CAMP), complement and acute-phase reactants (C3, CFH, SERPINA1), and oxidative stress and endothelial injury markers (PRDX1, APOE, HP, HPX). The concurrent elevation of adaptive immune components (IGHG1–4, IGHA1, B2M) suggests chronic immune activation with sustained antibody production and immune complex turnover. Collectively, these findings reflect an ongoing interplay between innate and adaptive immune pathways, oxidative stress, and vascular permeability—consistent with ongoing immune activation consistent with persistent antigenic exposure and endothelial dysfunction rather than renal pathology. Similar urinary proteomic patterns have been reported in conditions of chronic immune activation and post-viral inflammatory syndromes, where increased glomerular leakage of plasma proteins occurs secondary to cytokine-driven endothelial disruption [35,36]. The identified proteins, particularly CFH and PRDX1, underscore complement overactivation and redox imbalance—mechanisms previously implicated in long-term sequelae following both infection and vaccination. Thus, the patient's proteomic profile substantiates a systemic inflammatory phenotype concordant with transcriptomic findings and the clinical course of post–mRNA vaccine inflammatory syndrome.

HLA predisposition analysis was also performed, and notably, this patient carries HLA-B*07:02 and HLA-DRB1*11:04, alleles that have been linked to aberrant immune activation and chronic inflammatory disease. HLA-B*07:02 (a class I allele) shapes $CD8^+$ T-cell responses to viral antigens; for example, it has been considered the most dominant allele in SARS-CoV-2-infected individuals [37]. Intriguingly, HLA-B07:02 can also present certain peptides independently of the normal TAP-dependent antigen-processing pathway, an unusual feature that might sustain antigen presentation even when viruses evade conventional processing [38]. Conversely, B07:02 has been implicated in autoimmunity: multiple sclerosis patients show an increased frequency of HLA-B7 and a dysregulated B07:02–restricted $CD8^+$ T-cell response to Epstein–Barr virus [39], suggesting that suboptimal clearance of this persistent mRNA peptides in

HLA-B7 carriers may contribute to chronic CNS inflammation. HLA-DRB1*11:04 (a class II allele) is likewise associated with immune-mediated pathology. It belongs to the HLA-DR11 family, which is a strong genetic risk factor for systemic juvenile idiopathic arthritis (an IL-1/IL-6–driven inflammatory disorder) [40], and the DRB111:04 variant in particular has been linked to systemic sclerosis [41]. Structural studies indicate that DRB111 alleles share unique peptide-binding groove features that can skew epitope presentation, potentially lowering the threshold for autoreactive $CD4^+$ T-cell activation when certain antigens persist. In the context of this patient's prolonged detection of spike protein and residual vaccine plasmid DNA, these HLA alleles provide a plausible immunogenetic backdrop for sustained inflammation [42], thereby driving a chronic inflammatory response in this post-vaccination setting.

Conclusion

To our knowledge, this case documents the most comprehensive molecular evidence of long-term persistence of multiple vaccine-derived components following COVID-19 mRNA vaccination. Spike protein, vaccine mRNA, and plasmid DNA fragments were all detected more than 3.5 years after the patient's final Pfizer–BioNTech COVID-19 mRNA vaccine dose—far exceeding the assumed biological lifespan of these molecules. These vaccine- and spike-related findings were generated across multiple independent laboratories at multiple time points using diverse analytical methodologies in both blood and tissue specimens, following an extensive and repeated diagnostic evaluation that included more than 40 emergency department visits, over 200 specialty encounters across 18 medical disciplines, more than 100 non-routine laboratory investigations, over 100 imaging and functional diagnostic studies, and systematic exclusion of underlying etiologic mechanisms across infectious, autoimmune, rheumatologic, endocrine, genetic, hematologic, malignant, toxic/medication-related, cardiovascular/vascular, metabolic, and primary neurologic domains. Molecular analyses spanning 852–1,364 days post-vaccination consistently demonstrated persistence of vaccine-derived components across serial blood and tissue sampling. Detection was achieved through orthogonal platforms—including high-sensitivity ELISA, automated immunohistochemistry with histopathologic correlation, RT-PCR, standard PCR with Sanger sequencing confirmation, whole-genome sequencing, transcriptomic profiling, and quantitative mass spectrometry—across plasma, circulating exosomes, peripheral blood mononuclear cells, urine, and serial truncal skin biopsies, demonstrating convergent molecular signals across independent technologies and biological compartments. Spike protein remained detectable in plasma, exosomes, and serial skin biopsies; vaccine-derived mRNA persisted within circulating exosomes; and plasmid DNA elements, including spike gene fragments, origins of replication, and the SV40 enhancer, were identified in both immune cells and somatic tissue. Serial serologic testing spanning 809–1,433 days post-vaccination demonstrated persistently elevated spike antibody levels with five separate nucleocapsid-negative results across three independent laboratories, and nucleocapsid protein was absent in all spike-positive tissue specimens. This sustained nucleocapsid negativity across both serologic and tissue analyses effectively rules out prior SARS-CoV-2 infection as the source of the detected spike protein and genetic material. The reproducible, multi-compartment detection of spike protein, spike mRNA sequences, and plasmid backbone elements extending beyond 3.5 years represents an unprecedented duration of molecular persistence following mRNA vaccination. Together, these findings demonstrate that vaccine-derived genetic material and its protein products can persist in vivo for years, challenging longstanding assumptions of rapid clearance and biological inertness.

Clinically, the patient developed a progressive, multi-organ syndrome—pulmonary emboli, MRI-confirmed myocarditis, neurocognitive impairment, gastrointestinal dysbiosis, and chronic dermatologic inflammation—mirroring the molecular evidence of persistent antigen exposure, endothelial dysfunction, and systemic immune activation. Multi-omic analysis further revealed structural genomic instability, redox and mitochondrial stress, endothelial activation, and a proteomic signature of chronic inflammation and vascular injury. The patient's immunogenetic background (HLA-B*07:02, HLA-DRB1*11:04) provides an additional framework for prolonged antigen presentation and heightened inflammatory responsiveness.

Combined, these results outline a unified biological model: long-term persistence of spike protein and vaccine-derived nucleic acids, combined with genomic dysregulation, may drive chronic immune stimulation, tissue inflammation, and multi-system dysfunction in a subset of individuals. While these findings require validation in larger cohorts with matched controls, they highlight critical gaps in our understanding of mRNA vaccine biodistribution, persistence, and long-term immunologic consequences.

While limited to a single patient, this case underscores the need for sustained clinical surveillance, rigorous molecular biomonitoring, and comprehensive longitudinal studies to determine the prevalence, mechanisms, and clinical relevance of persistent vaccine-derived components. A re-evaluation of current assumptions regarding mRNA vaccine clearance, stability, and systemic impact is warranted to guide management of individuals presenting with chronic, unexplained post-vaccination symptoms.

Methods

Preparation of plasma and peripheral blood mononuclear cell (PBMC) fraction

Freshly isolated human EDTA whole blood (at least 5 ml) was layered in 15 ml conical centrifuge tubes at room temperature on top of 5 ml of Histopaque-1077 (Sigma-Aldrich #H8889). The samples were centrifuged at 400 × g for 30 minutes at room temperature in a swing-out centrifuge with no break. The top layer (plasma) was collected and frozen for further processing. The white, cellular PBMC layer at the plasma-density gradient interface was pipetted, transferred to an Eppendorf tube, and centrifuged at 250 × g for 10 minutes. It was then washed twice with phosphate buffer solution. The PBMC pellet was lysed in lysis buffer (20 mM Tris-HCl, 10 mM EDTA, 1% NP40, 1% Triton X-100, pH 7.4) for 30 min at 4 °C.

Exosome isolation

Exosomes were isolated using exosome precipitation solution (Macherey-Nagel #740398) by mixing 1 ml of plasma with 400 µl of exosome precipitation solution according to the manufacturer's instructions. The resulting exosome pellet was either lysed in 20 mM Tris-HCl, 10 mM EDTA, 1% NP40, 1% Triton X-100, pH 7.4, for 30 min at 4 °C to obtain the protein fraction, or further processed for RNA or DNA isolation.

Spike protein ELISA and IgG4 antibody detection

The concentration of spike protein in plasma, exosomes, and PBMCs was determined from protein fractions using enzyme-linked immunosorbent assay (ELISA) (Meso Scale Discovery). The IgG4 antibody titer against spike protein in plasma was quantified using Acro Biosystems ELISA (#RAS-T017) according to the manufacturer's protocols.

DNA and RNA extraction from tissues, exosomes and PBMC

Formalin-fixed tissue in paraffin blocks was sectioned into five 10 µm thick sections, mounted on Superfrost Plus slides, and air-dried overnight or longer. After paraffin removal and rehydration of the tissue sections in phosphate-buffered saline for 48 hours, the tissue was transferred to an Eppendorf tube and the fluid was completely discarded by centrifugation.

Total RNA was extracted from exosomes, PBMC, or tissue using the NucleoSpin RNA Plus XS Kit or the NucleoSpin Total RNA FFPE XS Kit with gDNA removal column (Macherey-Nagel #74099, #740969) according to the manufacturer's instructions. During this procedure, an additional DNase I treatment step was included for 15 minutes at room temperature to remove residual plasmid DNA fragments. The RNA was transcribed into cDNA (Applied Biosystems #4387406), and gene expression analysis was performed by polymerase chain reaction (PCR).

Plasmid DNA was extracted from exosomes and PBMC using the GeneJet Plasmid Miniprep Kit (Thermo Scientific). Genomic DNA was isolated either from formalin-fixed, paraffin-embedded tissue sections or from PBMC by isopropanol precipitation. In short, tissues were lysed with proteinase K in TES buffer (50 mM Tris-HCl, 100 mM EDTA, 100 mM NaCl, 1% SDS, pH 8.0) for 3–5 hours at 56 °C. After the addition of 6 M NaCl, the solutions were vortexed and centrifuged for 5 min to obtain a clear solution, which was then further treated with isopropanol. The genomic DNA was precipitated by centrifugation (15 min; 13,000 rpm), washed with 70% ethanol, air-dried, and eluted in water.

Gene expression analysis

Gene expression analysis was performed using polymerase chain reaction with Taq polymerase (Biozym #331610) and the following primers:

Spike protein sequence 1 (221bp)	**fw CCTACACCAACAGCTTTACC** **rev GATGTTGGACTTCTCGGTGC**
Spike protein sequence 2 (251bp)	**fw ACGTGGTCAACCAGAATGCC** **rev CACACACTCAGACATCTTGG**

Spike protein sequence 3 (362bp)	**fw GAACTTCAACTTCAACGGCC** **rev AGCTATTGTTCACGTGCTCG**
Replication of origin sequence 1 (105bp)	**fw CTACATACCTCGCTCTGCTAATC** **rev GCGCCTTATCCGGTAACTATC**
Replication of origin sequence 2 (204bp)	**fw CTACATACCTCGCTCTGCTAATC** **rev CGCTTTCTCATAGCTCACGC**
SV40 enhancer sequence (311bp)	**fw CCAGCTGTGGAATGTGTGTC** **rev GCTGACTAATTGAGATGCATGC**

A vial containing batch GH9715 was used as a positive control, as plasmid DNA from this batch was already isolated and sequenced and confirmed to refer to the plasmid sequence BNT162b2 (GenBank PP544445.1, GenBank PP544446.1, GenBank MQ287666.1 representing sequence 16 from patent WO2021214204). The PCR reactions were loaded onto a 2% agarose gel with ethidium bromide.

Routine Histology

Formalin-fixed tissues were routinely processed and paraffin-embedded tissues were cut into 5 µm sections and stained with hematoxylin and eosin (H&E) for histopathological examination.

Immunohistochemistry

Immunohistochemical staining was performed on the skin biopsies, using a fully automated immunostaining system (Ventana Benchmark, Roche). An antigen retrieval (Ultra CC1, Roche Ventana) was used for both antibodies. Incubation with the primary antibody (SARS-CoV-2 spike protein subunit 1, ProSci, #9083 and SARS-CoV-2 nucleocapsid protein, ProSci, #35-720) was carried out for 30 min in each case. Cultured cells that had been transfected *in vitro* served as a positive control for the detection of vaccine-induced spike protein expression and as a negative control for the detection of nucleocapsid protein (data not shown). The slides were examined with a light microscope (Nikon ECLIPSE 80i) and representative images were captured by the camera system Motic Europe Motic MP3.

Sample Collection and Shipment

Punch biopsy specimens were obtained from truncal skin within areas of clinically active Grover's disease prior to blood collection due to the time-sensitive handling requirements of blood-based assays. Blood specimens required receipt by the testing laboratory within 48–72 hours and were shipped on the day of collection. Formalin-fixed tissue biopsies are comparatively stable and were shipped with blood samples when feasible or separately when blood testing was not being conducted. All shipments used insulated packaging with ice packs for passive temperature maintenance and sealed secondary containment. All blood samples were delivered within two days of shipment.

Blood samples were collected on May 7, 2025 (Blood Sample 1) and August 26, 2025 (Blood Sample 2) and shipped on the day of collection. Tissue biopsy specimens were collected on April 24, 2025 (Tissue Sample 1), July 22, 2025 (Tissue Sample 2), and November 14, 2025 (Tissue Sample 3). Tissue Sample 1 was shipped with Blood Sample 1, Tissue Sample 2 was shipped with Blood Sample 2, and Tissue Sample 3 was shipped separately immediately following collection.

References

1. Ho, R.J.Y. Warp-Speed Covid-19 Vaccine Development: Beneficiaries of Maturation in Biopharmaceutical Technologies and Public-Private Partnerships. *Journal of Pharmaceutical Sciences* **2021**, *110*, 615-618, doi:10.1016/j.xphs.2020.11.010.
2. Parry, P.I.; Lefringhausen, A.; Turni, C.; Neil, C.J.; Cosford, R.; Hudson, N.J.; Gillespie, J. 'Spikeopathy': COVID-19 Spike Protein Is Pathogenic, from Both Virus and Vaccine mRNA. *Biomedicines* **2023**, *11*, 2287, doi:10.3390/biomedicines11082287.
3. Von Ranke NL, Zhang W, Anokhin P, et al. Synthetic messenger RNA vaccines and transcriptomic dysregulation: Evidence from new-onset adverse events and cancers post-vaccination. *World J Exp Med*. 2025;15(4):113869. Published 2025 Dec 20. doi:10.5493/wjem.v15.i4.113869
4. Ota, N.; Itani, M.; Aoki, T.; Sakurai, A.; Fujisawa, T.; Okada, Y.; Noda, K.; Arakawa, Y.; Tokuda, S.; Tanikawa, R. Expression of SARS-CoV-2 spike protein in cerebral Arteries: Implications for hemorrhagic stroke Post-mRNA vaccination. *Journal of Clinical Neuroscience* **2025**, *136*, 111223, doi:10.1016/j.jocn.2025.111223.
5. Krauson, A.J.; Casimero, F.V.C.; Siddiquee, Z.; Stone, J.R. Duration of SARS-CoV-2 mRNA vaccine persistence and factors associated with cardiac involvement in recently vaccinated patients. *npj Vaccines* **2023**, *8*, doi:10.1038/s41541-023-00742-7.
6. Luo, J.; Molbay, M.; Chen, Y.; Horvath, I.; Kadletz, K.; Kick, B.; Zhao, S.; Al-Maskari, R.; Singh, I.; Ali, M.; et al. Nanocarrier imaging at single-cell resolution across entire mouse bodies with deep learning. *Nature Biotechnology* **2025**, doi:10.1038/s41587-024- 02528-1.
7. Patterson, B.K.; Yogendra, R.; Francisco, E.B.; Guevara-Coto, J.; Long, E.; Pise, A.; Osgood, E.; Bream, J.; Kreimer, M.; Jeffers, D.; et al. Detection of S1 spike protein in CD16+ monocytes up to 245 days in SARS-CoV-2-negative post-COVID-19 vaccine syndrome (PCVS) individuals. *Human Vaccines & Immunotherapeutics* **2025**, *21*, doi:10.1080/21645515.2025.2494934.
8. Mead, M.N. Myocarditis after SARS-CoV-2 infection and COVID-19 vaccination: Epidemiology, outcomes, and new perspectives. *International Journal of Cardiovascular Research & Innovation* **2025**, doi:10.61577/ijcri.2025.100001.
9. Hazan, S.; Dave, S.; Barrows, B.; Borody, T.J. S2099 Persistent Damage to the Gut Microbiome Following Messenger RNA SARS-CoV-2 Vaccine. *American Journal of Gastroenterology* **2022**, *117*, e1429-e1430, doi:10.14309/01.ajg.0000865036.78992.16.
10. Centers for Disease Control and Prevention. *Interim Guidelines for COVID-19 Antibody Testing.* Updated December 16, 2022. CDC. https://archive.cdc.gov/www_cdc_gov/coronavirus/2019-ncov/hcp/testing/antibody-tests-guidelines.html. Accessed January 30, 2026.
11. Bolze, A.; Neveux, I.; Schiabor Barrett, K.M.; White, S.; Isaksson, M.; Dabe, S.; Lee, W.; Grzymski, J.J.; Washington, N.L.; Cirulli, E.T. HLA-A∗03:01 is associated with increased risk of fever, chills, and stronger side effects from Pfizer-BioNTech COVID-19 vaccination.
12. Yasuda, S.; Suzuki, S.; Yanagisawa, S.; Morita, H.; Haisa, A.; Satomura, A.; Nakajima, R.; Oikawa, Y.; Inoue, I.; Shimada, A. HLA typing of patients who developed subacute thyroiditis and Graves' disease after SARS-CoV-2 vaccination: a case report. *BMC Endocrine Disorders* **2023**, *23*, 54, doi:10.1186/s12902-023-01287-5.
13. Bianco, A.; Di Sante, G.; Colò, F.; De Arcangelis, V.; Cicia, A.; Del Giacomo, P.; De Bonis, M.; Morganti, T.G.; Carlomagno, V.; Lucchini, M.; et al. Multiple Sclerosis Onset before and after COVID-19 Vaccination: Can HLA Haplotype Be Determinant? *International Journal of Molecular Sciences* **2024**, *25*, doi:10.3390/ijms25084556.
14. Magri, C.A.-O.; Marchina, E.; Sansone, E.; D'Adamo, A.P.; Cappellani, S.; Bonfanti, C.; Terlenghi, L.; Biasiotto, G.; Zanella, I.; Sala, E.; et al. Genome-wide association studies of response and side effects to the BNT162b2 vaccine in Italian healthcare workers: Increased antibody levels and side effects in carriers of the HLA-A*03:01 allele.
15. Hulscher, N.; Procter, B.C.; Wynn, C.; McCullough, P.A. Clinical Approach to Post- acute Sequelae After COVID-19 Infection and Vaccination. *Cureus* **2023**, doi:10.7759/cureus.49204.

16. Hulscher, N.; Bowden, M.; McCullough, P. Review: Calls for Market Removal of COVID-19 Vaccines Intensify as Risks Far Outweigh Theoretical Benefits. **2025**, *6*.
17. Aldén, M.; Olofsson Falla, F.; Yang, D.; Barghouth, M.; Luan, C.; Rasmussen, M.; De Marinis, Y. Intracellular Reverse Transcription of Pfizer BioNTech COVID-19 mRNA Vaccine BNT162b2 In Vitro in Human Liver Cell Line. *Current Issues in Molecular Biology* **2022**, *44*, 1115-1126, doi:10.3390/cimb44030073.
18. Anthony M. Kyriakopoulos, P.A.M., Greg Nigh, Stephanie Seneff. Potential Mechanisms for Human Genome Integration of Genetic Code from SARS-CoV-2 mRNA Vaccination: Implications for Disease. *Neurological Disorders* **2022**, *10*, doi:10.4172/2329- 6895.10.10.519.
19. Catanzaro JA, Hulscher N, McCullough PA. Genomic Integration and Molecular Dysregulation in Aggressive Stage IV Bladder Cancer Following COVID-19 mRNA Vaccination. Int J Innov Res Med Sci. 2025;10(10):380-386. doi:10.23958/ijirms/vol10-i10/2130.
20. European Medicines Agency. *Comirnaty: COVID-19 mRNA vaccine (nucleoside-modified). Assessment report.* EMA/707383/2020 Corr.2. Published February 19, 2021. Updated October 20, 2023. Accessed January 30, 2026.
21. Burbelo, P.D.; Riedo, F.X.; Morishima, C.; Rawlings, S.; Smith, D.; Das, S.; Strich, J.R.; Chertow, D.S.; Davey, R.T.; Cohen, J.I. Sensitivity in Detection of Antibodies to Nucleocapsid and Spike Proteins of Severe Acute Respiratory Syndrome Coronavirus 2 in Patients With Coronavirus Disease 2019. *The Journal of Infectious Diseases* **2020**, *222*, 206-213, doi:10.1093/infdis/jiaa273.
22. Sutanto, H.; Soegiarto, G. Risk of Thrombosis during and after a SARS-CoV-2 Infection: Pathogenesis, Diagnostic Approach, and Management. *Hematology Reports* **2023**, *15*, 225-243, doi:10.3390/hematolrep15020024.
23. Rogers, C.; Thorp, J.; Cosgrove, K.; McCullough, P. COVID-19 Vaccines: A Risk Factor for Cerebral Thrombotic Syndromes. *International Journal of Innovative Research in Medical Science* **2024**, *9*, 621 - 627, doi:10.23958/ijirms/vol09-i11/1982.
24. CDC. Clinical Considerations: Myocarditis and Pericarditis after Receipt of COVID-19 Vaccines Among Adolescents and Young Adults. **2023**.
25. Faksova, K.; Walsh, D.; Jiang, Y.; Griffin, J.; Phillips, A.; Gentile, A.; Kwong, J.C.; Macartney, K.; Naus, M.; Grange, Z.; et al. COVID-19 vaccines and adverse events of special interest: A multinational Global Vaccine Data Network (GVDN) cohort study of 99 million vaccinated individuals. *Vaccine* **2024**, *42*, 2200-2211, doi:10.1016/j.vaccine.2024.01.100.
26. Schauer, J.; Buddhe, S.; Gulhane, A.; Sagiv, E.; Studer, M.; Colyer, J.; Chikkabyrappa, S.M.; Law, Y.; Portman, M.A. Persistent Cardiac Magnetic Resonance Imaging Findings in a Cohort of Adolescents with Post-Coronavirus Disease 2019 mRNA Vaccine Myopericarditis. *The Journal of Pediatrics* **2022**, *245*, 233-237, doi:10.1016/j.jpeds.2022.03.032.
27. McCullough, P.A.; Hulscher, N. Risk stratification for future cardiac arrest after COVID- 19 vaccination. *World Journal of Cardiology* **2025**, *17*, doi:10.4330/wjc.v17.i2.103909.
28. Paardekooper, C. How Bad is My Batch? Available online: https://knollfrank.github.io/HowBadIsMyBatch/HowBadIsMyBatch.html
29. Brogna, C.; Cristoni, S.; Marino, G.; Montano, L.; Viduto, V.; Fabrowski, M.; Lettieri, G.; Piscopo, M. Detection of recombinant Spike protein in the blood of individuals vaccinated against SARS-CoV-2: Possible molecular mechanisms. *PROTEOMICS – Clinical Applications* **2023**, *17*, doi:10.1002/prca.202300048.
30. Bhattacharjee, B.; Lu, P.; Monteiro, V.S.; Tabachnikova, A.; Wang, K.; Hooper, W.B.; Bastos, V.; Greene, K.; Sawano, M.; Guirgis, C.; et al. Immunological and Antigenic Signatures Associated with Chronic Illnesses after COVID-19 Vaccination. **2025**, doi:10.1101/2025.02.18.25322379.
31. Liu, B.; Conroy, J.M.; Morrison, C.D.; Odunsi, A.O.; Qin, M.; Wei, L.; Trump, D.L.; Johnson, C.S.; Liu, S.; Wang, J. Structural variation discovery in the cancer genome using next generation sequencing: computational solutions and perspectives.
32. Eleveld, T.A.-O.; Ylstra, B.A.-O.; Looijenga, L.H.J. Low-amplitude copy number gains shape cancer through known and novel oncogenes with associated therapeutic vulnerabilities. LID - 10.1093/nar/gkaf689 [doi] LID - gkaf689.
33. Patkar, S.; Heselmeyer-Haddad, K.; Auslander, N.; Hirsch, D.; Camps, J.; Bronder, D.; Brown, M.; Chen, W.-D.; Lokanga, R.; Wangsa, D.; et al. Hard wiring of normal tissue- specific chromosome-wide gene expression levels is an additional factor driving cancer type-specific aneuploidies. *Genome Medicine* **2021**, *13*, 93, doi:10.1186/s13073-021- 00905-y.

34. Zhang, C.-Z.; Spektor, A.; Cornils, H.; Francis, J.M.; Jackson, E.K.; Liu, S.; Meyerson, M.; Pellman, D. Chromothripsis from DNA damage in micronuclei. *Nature* **2015**, *522*, 179-184, doi:10.1038/nature14493.
35. Joshi, N.; Garapati, K.; Ghose, V.; Kandasamy, R.K.; Pandey, A. Recent progress in mass spectrometry-based urinary proteomics. *Clinical Proteomics* **2024**, *21*, doi:10.1186/s12014-024-09462-z.
36. Zhao, M.; Li, M.; Yang, Y.; Guo, Z.; Sun, Y.; Shao, C.; Li, M.; Sun, W.; Gao, Y. A comprehensive analysis and annotation of human normal urinary proteome. *Scientific Reports* **2017**, *7*, doi:10.1038/s41598-017-03226-6.
37. Peng, Y.; Felce, S.L.; Dong, D.; Penkava, F.; Mentzer, A.J.; Yao, X.; Liu, G.; Yin, Z.; Chen, J.-L.; Lu, Y.; et al. An immunodominant NP105–113-B*07:02 cytotoxic T cell response controls viral replication and is associated with less severe COVID-19 disease. *Nature Immunology* **2021**, *23*, 50-61, doi:10.1038/s41590-021-01084-z.
38. de la Salle, H.; Houssaint, E.; Peyrat, M.A.; Arnold, D.; Salamero, J.; Pinczon, D.; Stevanovic, S.; Bausinger, H.; Fricker, D.; Gomard, E.; et al. Human peptide transporter deficiency: importance of HLA-B in the presentation of TAP-independent EBV antigens. *The Journal of Immunology* **1997**, *158*, 4555-4563, doi:10.4049/jimmunol.158.10.4555.
39. Jilek, S.; Schluep, M.; Harari, A.; Canales, M.; Lysandropoulos, A.; Zekeridou, A.; Pantaleo, G.; Du Pasquier, R.A. HLA-B7–Restricted EBV-Specific CD8+ T Cells Are Dysregulated in Multiple Sclerosis. *The Journal of Immunology* **2012**, *188*, 4671-4680, doi:10.4049/jimmunol.1103100.
40. Ombrello, M.J.; Remmers, E.F.; Tachmazidou, I.; Grom, A.; Foell, D.; Haas, J.-P.; Martini, A.; Gattorno, M.; Özen, S.; Prahalad, S.; et al. HLA-DRB1*11and variants of the MHC class II locus are strong risk factors for systemic juvenile idiopathic arthritis. *Proceedings of the National Academy of Sciences* **2015**, *112*, 15970-15975, doi:10.1073/pnas.1520779112.
41. Machhua, S.; Sharma, S.K.; Kumar, Y.; Singh, S.; Aggarwal, R.; Anand, S.; Kumar, M.; Singh, H.; Minz, R.W. Human leukocyte antigen association in systemic sclerosis patients: our experience at a tertiary care center in North India. *Frontiers in Immunology* **2023**, *14*, doi:10.3389/fimmu.2023.1179514.
42. Georgopoulos, A.; James, L.; Peterson, P. Human Leukocyte Antigen (HLA) at the Root of Persistent Antigens and Long COVID. *Journal of Immunological Sciences* **2025**, *9*, 1- 3, doi:10.29245/2578-3009/2025/1.1257.

SUPPLEMENTARY MATERIAL

Table S1. Innate Immune Activation (Neutrophil and Macrophage Signaling). Legend: PSM (Peptide-Spectrum Match) reflects the number of detected peptide fragments for each protein. **Abundance Ratio (EVs / Urine)** indicates protein enrichment in urinary extracellular vesicles relative to whole urine, and **Adjusted P-value** denotes the statistical significance of this difference after multiple-testing correction.

Gene	Description	PSM	Abundance Ratio	Abundance Ratio Adj. P-Value
S100A8	Proinflammatory calcium-binding protein; activates TLR4 and RAGE signaling.	704	5.709	0.84659819
S100A9	Partner of S100A8; promotes neutrophil chemotaxis and cytokine release.	457	5.922	0.83834255
S100A12	Induces endothelial activation via RAGE; amplifies innate inflammation.	112	9.82	0.74715833
CD14	LPS co-receptor for TLR4; initiates innate immune activation.	60	5.061	0.86160805
CAMP	Antimicrobial peptide LL-37; recruits neutrophils and modulates cytokines.	127	10.542	0.72460914
LTF	Lactoferrin; antimicrobial and anti-inflammatory iron-binding glycoprotein.	653	10.435	0.72865898
HP	Haptoglobin; scavenges free hemoglobin to limit oxidative inflammation.	280	0.229	0.49508305
HPX	Hemopexin; binds free heme to reduce ROS-mediated inflammation.	129	0.54	0.75760585
GSN	Gelsolin; controls actin release and dampens inflammatory cascades.	299	2.011	0.98343522
ORM1	Orosomucoid 1; acute phase reactant modulating neutrophil adhesion.	96	0.049	0.09312903
ANXA1	Annexin A1; glucocorticoid-induced, promotes resolution of inflammation.	58	13.225	0.65892721
ANXA2	Regulates membrane repair and macrophage cytokine signaling.	84	6.406	0.82775716
PIGR	Transports IgA/IgM across mucosa; bridges innate and mucosal defense.	279	0.845	0.83937768

Table S2. Complement and Acute-Phase Response. Legend: PSM (Peptide-Spectrum Match) reflects the number of detected peptide fragments for each protein. **Abundance Ratio (EVs / Urine)** indicates protein enrichment in urinary extracellular vesicles relative to whole urine, and **Adjusted P-value** denotes the statistical significance of this difference after multiple-testing correction.

Gene	Description	PSM	Abundance Ratio	Abundance Ratio Adj. P-Value
C3	Central complement component; promotes opsonization and inflammation.	221	6.668	0.86104676
CFH	Complement factor H; inhibits excessive alternative pathway activation.	69	8.563	0.49508305
CFI	Complement factor I; degrades activated C3b and C4b to prevent self-damage.	70	2.535	0.75760585
SERPINA1	α1-antitrypsin; protects tissues from neutrophil elastase.	292	0.308	0.86104676
SERPINA3	Acute-phase serine protease inhibitor; modulates inflammation.	106	1.966	0.97499333
SERPING1	C1 inhibitor; prevents spontaneous activation of complement cascade.	153	4.309	0.79175269
MASP2	Lectin pathway activator; initiates C4/C2 cleavage.	70	0.172	0.65892721
FGA	Fibrinogen alpha chain; marker of systemic inflammation.	191	3.167	0.97077855
FGB	Fibrinogen beta chain; involved in coagulation and inflammothrombosis.	147	4.792	0.09346852
FGG	Fibrinogen gamma chain; supports platelet aggregation during inflammation.	191	8.724	0.86104676
A2M	Broad-spectrum protease inhibitor regulating complement and cytokine activity.	119	0.53	0.49508305
ORM1	Acute phase glycoprotein involved in inflammatory response modulation.	96	0.049	0.75760585

Table S3. Oxidative Stress–Linked Inflammation. Legend: PSM (Peptide-Spectrum Match) reflects the number of detected peptide fragments for each protein. **Abundance Ratio (EVs / Urine)** indicates protein enrichment in urinary extracellular vesicles relative to whole urine, and **Adjusted P-value** denotes the statistical significance of this difference after multiple-testing correction.

Gene	Description	PSM	Abundance Ratio	Abundance Ratio Adj. P-Value
PRDX1	Peroxiredoxin 1; antioxidant enzyme mitigating ROS during inflammation.	66	5.147	0.86104676
HP	Reduces oxidative stress by binding free hemoglobin.	280	0.229	0.49508305
HPX	Scavenges heme, preventing oxidative endothelial injury.	129	0.54	0.75760585
APOE	Modulates macrophage activation and lipid-associated oxidative inflammation.	108	5.321	0.86104676
APOA1	Anti-inflammatory HDL component with antioxidant properties.	192	1.858	0.97499333
APOA4	Regulates lipid metabolism and oxidative balance in inflammation.	276	7.992	0.79175269

ANXA1	Promotes resolution phase and reduces ROS-induced damage.	58	13.225	0.65892721
EFEMP1	ECM-associated regulator of oxidative signaling in tissue stress.	160	1.768	0.97077855
PTGDS	Produces prostaglandin D2; regulates oxidative and inflammatory balance.	463	0.05	0.09346852

Table S4. Adaptive Antibody-Mediated Regulation. Legend: PSM (Peptide-Spectrum Match) reflects the number of detected peptide fragments for each protein. **Abundance Ratio (EVs / Urine)** indicates protein enrichment in urinary extracellular vesicles relative to whole urine, and **Adjusted P-value** denotes the statistical significance of this difference after multiple-testing correction.

Gene	Function	PSM	Abundance Ratio	Abundance Ratio Adj. P-Value
IGHG1	Immunoglobulin heavy chain gamma 1; mediates adaptive immune response.	396	1.153	0.89379678
IGHG2	Immunoglobulin gamma 2; complement-fixing antibody subtype.	493	0.419	0.70285101
IGHG3	Immunoglobulin gamma 3; potent complement activator.	270	3.147	0.96043029
IGHG4	Non-complement-fixing IgG; modulates chronic immune activation.	89	1.004	0.87059901
IGHA1	Secretory IgA heavy chain; protects mucosal surfaces.	182	0.517	0.75721935
IGHA2	Secondary IgA subtype; maintains mucosal immune tolerance.	80	3.457	0.94332212
IGHM	IgM heavy chain; early adaptive immune response antibody.	132	1.045	0.87549605
IGKC	Immunoglobulin kappa constant; light chain for antibody assembly.	159	0.558	0.76189784
IGLC2	Lambda light chain; component of adaptive antibodies.	82	0.762	0.82775716
IGLL5	Immunoglobulin lambda-like polypeptide 5; involved in B-cell signaling.	94	0.44	0.71565047
B2M	Beta-2 microglobulin; component of MHC I, reflects immune activation.	115	0.818	0.83474445
CD55	Decay accelerating factor; protects cells from complement-mediated lysis.	117	0.025	0.03422473
CD59	Inhibits membrane attack complex formation; prevents autologous injury.	204	0.045	0.08269538
PIGR	Links mucosal antibody secretion to innate defense.	279	0.845	0.83937768